Regional Studies in Marine Science 85 (2025) 104143

Contents lists available at ScienceDirect

Regional Studies in Marine Science

journal homepage: www.elsevier.com/locate/rsma

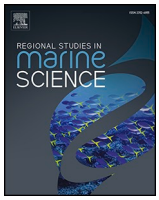

A prospective study on the biodegradation of petroleum hydrocarbons mediated by selected marine bacterial isolates

Umaima Hamed Al Hoqani [a,*], Syed Najmul Hejaz Azmi [a], Jayachandran Vavolil P [a], Huda Sultan Al Habsi [a], Salla Hemadri Reddy [a,b], Pankaj Sah [a], Jokha Salim Al Harthi [a], Zainab Nasser Bani Saad [a], Zainab Saif Al Nabhani [a], Qamar Uddin Ahmed [c], Md. Abdur Rashid Mia [d], Kamal Abdelrahman [e], Mohammed S. Fnais [e]

[a] *Applied Sciences Department, College of Applied Sciences and Pharmacy, University of Technology and Applied Sciences, P. O. Box 74, Al Khuwair, Muscat 133, Sultanate of Oman*
[b] *Biomedical Sciences Department, School of Health Sciences, Apollo University, Saketa, Murukambattu, Chittoor District, Andhra Pradesh, India*
[c] *Drug Discovery and Synthetic Chemistry Research Group, Department of Pharmaceutical Chemistry, Kulliyyah of Pharmacy, International Islamic University Malaysia (IIUM), Kuantan, Pahang Darul Makmur 25200, Malaysia*
[d] *Cooperative Research, Extension, and Education Services (CREES), Northern Marianas College, P.O. Box 501250, Saipan, MP 96950, USA*
[e] *Department of Geology & Geophysics, College of Science, King Saud University, P. O. Box 2455, Riyadh 11451, Saudi Arabia*

ARTICLE INFO

Keywords:
Hydrocarbon-degrading bacteria
Marine ecosystem
N-alkanes
Biodegradation
Niallia
GC-MS

ABSTRACT

Petroleum hydrocarbons are an indispensable energy source and serve as a fundamental feedstock for petroleum oil refiners and petrochemical industries. The release of petroleum hydrocarbon pollutants into the environment is associated with anthropogenic activities during crude oil production, exploration, and transportation. The widespread petroleum hydrocarbons pollutants in the environment caused a major concern due to their bio-accumulation potential and harmful effect on the ecosystem. Nevertheless, such polluted environment with petroleum hydrocarbons is enriched with microorganisms that have the natural ability to utilize the petroleum hydrocarbons as a carbon source for their growth and metabolic activities. Therefore, this study focused on the isolation, molecular identification and characterization of bacterial isolates from seawater samples collected at the coastal area nearby oil Refinery Company in Oman. Six marine bacteria were isolated from the contaminated seawater and their taxonomical identification was performed based on 16S rRNA gene sequence. The degradation potential of bacterial isolates was assessed by growing them in F/2 medium supplemented with crude oil as a sole carbon source. Two bacterial isolates belonging to the genus *Niallia* showed the strongest growth (S1.5: 1.01 ± 0.27 and S2.1: 0.88 ± 0.23) and were subjected to further Gas Chromatography–Mass Spectrometry (GC-MS) analysis determining which n-alkanes in crude oil were degraded by the isolates. The GC-MS chromatogram indicated that S2.1 exhibited greater efficiency in degrading a higher number of carbon n-alkanes (C13-C34) com-pared to S1.5 (C13-C18). The t-test analysis confirmed the efficiency of S2.1 ($t = 3.182$; $p < 0.01$) (93.61 ± 1.48 %) compared to S1.5 (86.08 ± 1.85 %). Molecular docking revealed robust binding affinities between selected n-alkanes and alkane hydroxylases, facilitating the subsequent degradation of n-alkanes in crude oil. The degradation potential of *Niallia* can be further exploited for the treatment of petroleum contaminated, especially with the incorporation of recent technological advancements.

1. Introduction

Crude oil is an essential resource for global industry but is also a significant source of pollution in terrestrial, atmospheric, and oceanic ecosystems. Factors such as rising population, modern lifestyles, and other influences, have led to increased exposure to petroleum hydrocarbons in our daily lives (Rajabi et al., 2020). The undeniable truth is that petroleum hydrocarbons can have detrimental effects on all forms of life (Saadoun, 2015). Anthropogenic activities, including accidental or deliberate discharges, operational spills from offshore pipelines, and

* Corresponding author.
E-mail address: Umaima.alhoqani@utas.edu.om (U.H. Al Hoqani).

https://doi.org/10.1016/j.rsma.2025.104143
Received 26 September 2024; Received in revised form 21 January 2025; Accepted 16 March 2025
Available online 21 March 2025

tankers, are the most evident causes of oil pollution in marine ecosystems.

Hydrocarbons enter the marine environment not merely as "wet" byproducts of oil but also as gaseous air pollutants. Non-methane volatile organic compounds are examples of hydrocarbons vapors released during various stages of extraction to consumption. Between 1970 and 2013, at least eight large oil spills, each exceeding 700 tons, were reported in the oceans (Saadoun, 2015). A report by the International Tanker Owners Pollution Federation Limited (ITOPF) highlighted that in 2021 alone, oil spills in Asia, Africa, and North America collectively contributed approximately 10,000 tons of oil pollution, underscoring of this issue in marine ecosystems (ITOPF, 2024).

Addressing oil spills in the marine environment can be challenging, but hydrocarbon-degrading bacteria have naturally evolved in petroleum-polluted environments. These bacteria utilize petroleum compounds as their carbon and energy sources, making them promising candidates for oil spill remediation (Xu et al., 2018). Bacteria possess exceptional versatility, allowing them to reach higher densities, tolerate harsh environmental conditions, and degrade noxious compounds, including petroleum hydrocarbons (Wang et al., 2019; Zheng et al., 2011).

In environmental cleanup, bioremediation strategy offers advantages such as reduced capital and operating costs compared to chemical and physical methods, while also being environmentally friendly. Utilizing microbial whole cells for bio-transformations provides additional advantages, including ease of culturing and maintaining cells, lower costs compared to enzyme extraction or purification, and the feasibility of obtaining biomass at a low cost (Xu et al., 2018).

In general, petroleum hydrocarbons are insoluble in water and are classified as volatile and non-volatile organic compounds. These hydrocarbons are present in crude oil and often found in surface and underground water as a result of industrial activities (Bouchard et al., 2008; Mohammadi et al., 2020; Rajabi et al., 2020). Due to their hydrophobic nature, many petroleum hydrocarbons exhibit a high affinity for organic matter, making them easily adsorbed onto organic matter, soil, and sediments. Once adsorbed, they can be difficult to remove and may persist for years before degrading (Xu et al., 2018). One factor contributing to the persistence of adsorbed petroleum hydrocarbons is the limited surface area, which reduce their bioavailability for biodegradation and limits access to the physical processes that could otherwise aid in their breakdown or dilution (Silliman et al., 2012).

Microbial populations carrying oil-degrading plasmids are increasingly observed in oil polluted environments (Atlas, 1995; Nwankwo and Okpokwasili, 2019). Various studies highlighted the significant role of plasmids in enabling bacterial adaptation within a population. These plasmids enhance the assembly and dissemination of polyaromatic hydrocarbons (PAH) catabolic gene clusters within the bacterial consortia (Dealtry et al., 2014). Knowing the genetics of the bacteria with degrading potential is pivotal, as it can pave the way to the safer and more cost-effective utilization of genetically engineered microbes (GEM) to enhance desired traits, rather than relying on alternative methods (Rafeeq et al., 2023; Sakshi et al., 2023).

The present study aimed to i) determine whether marine bacteria isolated from petroleum-contaminated seawater in Oman can degrade the petroleum hydrocarbons by growing them in a medium supplemented with crude oil serve as the sole carbon source, ii) characterize these bacterial isolates based on 16S rRNA gene sequence, iii) evaluate the n-alkanes degradation capabilities of the most effective bacterial isolates i.e. S1.5 and S2.1, and iv) simulate the binding affinity between selected n-alkanes (C13, C18 and C34) against the target alkane hydroxylases -i.e. non-heme iron monooxygenase (AlkB) and long-chain alkane monooxygenase (LadA) as key enzymes in the initial stage of hydrocarbon catabolism during aerobic degradation. The novelty of this study lies in isolation of two bacterial isolates S1.5 and S2.1 with promising biodegradation potential from *Niallia* genus. This genus was proposed in 2020 for which only a few studies have been reported so far in the context of bioremediation.

2. Materials and methods

2.1. Collection of oil contaminated seawater samples

Oil contaminated seawater samples were collected from two locations at a coastal area nearby Petroleum Development Oman (PDO) at Mina Al-Fahal; location 1 (23°38'13.7" N and 58°30'26.7" E) and location 2 (23°37'55.6" N and 58°30'52.6" E). The water samples were collected in sterilized bottles and stored in the laboratory at room temperature for further investigation.

2.2. Preparation of F/2 liquid medium

Stock solutions 1, 2 and 3 were used for preparation of F/2 medium with minor modification according to the previous studies (Guillard and Hargraves, 1993; Radakovits et al., 2012; Rodrigues and de Carvalho, 2022). Stock solution 1 was prepared by dissolving 3.15 g $FeCl_3.6H_2O$, 4.36 g $Na_2EDTA.2H_2O$, 0.18 g $MnCl_2.4H_2O$, 0.023 g $ZnSO_4.7H_2O$, 0.0025 g $CuSO_4.5H_2O$, 0.022 g $Na_2MoO_4.2H_2O$ and 0.0026 g $CoCl_2.7H_2O$ in 1 L distilled water. All these metallic salts were soluble in water and did not cause any precipitation when mixed with distilled water. The mixture was autoclaved at 121 °C and 15 psi. The stock solution 2 was prepared by dissolving 7.5 g $NaNO_3$ and 0.566 g $NaH_2PO_4.2H_2O$ in 1 L distilled water. The stock solution was autoclaved at 121°C and 15 psi. The stock solution 3 (1 M Tris(hydroxymethyl)aminomethane or in short Tris) was prepared by dissolving 12.11 g Tris in 100 mL distilled water and the solution was autoclaved at 121°C and 15 psi. In addition to these stock solutions, vitamin solutions of B12 (0.005 g B12 in 100 mL distilled water) and Thiamine HCl (0.01 g of Thiamine HCl in 100 mL distilled water) were prepared. Both solutions were filtered using 0.25 μm Millipore filter and stored at −20°C. The F/2 medium was prepared by transferring 1 mL of stock solution 1 and 10 mL of stock solution 2 in 900 mL filtered and autoclaved seawater in 1 L standard volumetric flask. The pH of the medium was adjusted to 6.8–7.0 using 1 M HCl or 1 M NaOH. The F/2 medium was autoclaved at 121°C and 15 psi. After autoclaving, 1 mL of stock solution 3, 0.1 mL B12 and 1.0 mL thiamine HCl were added into F/2 medium. The F/2 medium solution was diluted up to the mark in 1 L standard volumetric flask with filtered and autoclaved seawater. The agar plates were prepared by adding 2 % (w/v) agar and then autoclaved at 121°C and 15 psi. The prepared medium was poured into the petri dishes.

2.3. Enrichment and isolation of hydrocarbon-degrading bacteria

Bacteria from seawater were enriched in an F/2 medium supplemented with 1 % (v/v) crude oil as the sole source of carbon (Abed et al., 2007). The enrichment was performed in a 250 mL conical flask containing 100 mL F/2 medium supplemented with 1 % (v/v) crude oil. The culture was maintained at 30 °C with constant shaking at 200 rpm. After a week of incubation, an aliquot of the cloudy culture was inoculated into fresh F/2 medium supplemented with 1 % v/v crude oil, and this step was repeated three times. Serial dilution and direct plating were used to obtain axenic culture. The bacteria isolated from the coastal area near ORPIC were labelled as S1.1, S1.2, S1.3, S1.4 and S1.5, while those from the coastal area near PDO were labelled as S2.1.

2.4. Isolation and molecular identification of bacterial strains

The nucleic acid extraction was carried out with cells of the bacterial isolates cultured in 5 mL nutrient broth and incubated overnight at 30 °C with constant shaking at 200 rpm (Innova 4300 incubator shaker, New Brunswick Scientific). The cells were harvested by centrifugation at 12,000 xg for 10 minutes. The genomic DNA was isolated from the cells using Thermo Scientific GeneJET Genomic DNA Purification Kit

according to the manufacturer's instructions. The amplification of 16S ribosomal RNA (16S rRNA) gene was performed in a 25 μL PCR reaction that contained: 1x Standard Taq Reaction Buffer (NEB), 1 unit of Taq DNA Polymerase (NEB, 10 mM of each deoxyribonucleotide triphosphate (dNTPs), 5 μM of each forward and reverse oligonucleotide primers (Macrogen Inc., Seoul, South Korea), ~2.5 ngμL^{-1} DNA template and ddH_2O to make the final volume 25 μL. The PCR reaction was performed in a Techne TC-3000X Thermal Cycler using bacterial universal primer pair 27 F 5' AGA GTT TGA TCC TGG CTC AG 3' and 1492 R 5' GGT TAC CTT GTT ACG ACT T 3' (Agunbiade et al., 2022).The cycle conditions employed to amplify the target region within 16S RNA gene were as follows: 94 °C for 1 min, 25 cycles of 94 °C for 30 s, 56 °C for 30 s, 72 °C for 1 min and final extension at 72 °C for 5 min. The PCR products were analyzed on a 1 % (w/v) agarose gel in TAE buffer (40 mM Tris, 20 mM acetic acid and 1 mM sodium EDTA) containing 1 μgmL^{-1} ethidium bromide. The PCR products were visualized on a UV transilluminator, and results were captured using UVP Gel Documentation System (UVP GelDoc-It2 310 Imaging System, Fisher Scientific). The size of fragments was estimated with reference to a Gene Ruler DNA ladder Mix (Thermo Scientific). The primers used were synthesized by Macrogen Inc., Seoul, South Korea. PCR products were purified using Gene Jet PCR purification kit (Thermo Scientific) as per the manufacturer's instructions. The purified PCR product at a DNA concentration of 1 ngμL^{-1} per 100 bp was sequenced using the Sanger sequencing method (Macrogen Inc., Seoul, South Korea). The results of the sequencing were analyzed using Sequencher 5.4.6 (Gene Codes Corp., Ann Arbor, MI, USA).

2.5. Phylogenetic analysis of 16S rRNA sequence

The obtained 16S rRNA sequences from the isolates were aligned with closely related sequences retrieved from NCBI database using Molecular Evolutionary Genetic Analysis (MEGA) 11 software. The phylogenetic tree with 1000 bootstrap replicates was constructed by applying a maximum likelihood method in MEGA 11 software (Tamura et al., 2021). The quality filtered 1300 bp consensus 16S rRNA gene sequences of the isolates from this study were deposited in Gene Bank at National Center for Biotechnology Information under the accession numbers PP346386- PP346391.

2.6. Assessment of bacterial growth with selected hydrocarbons

To test the ability of the strains to grow with selected hydrocarbons – namely, n-hexane, n-octane and toluene as a sole carbon sources (Kothari, 1963), cells from a 5 mL overnight grown culture were washed twice with sterile 0.85 % NaCl solution and then the cells were streaked on 2 % F/2 agar plates. A plain 2 % F/2 agar plate was included as a control. For the utilization of n-hexane by the isolates, the streaked 2 % F/2 agar plates (not upside down) were kept in a desiccator containing 10 mL n-hexane and 90 mL hexadecane in a 100 mL beaker. The control plates were also kept inside this desiccator. The plates were incubated at 25 °C for 14 days. Similarly, the utilization studies of n-octane and toluene were performed by placing the streaked 2 % F/2 agar plates and control plates in a desiccator containing 20 mL n-octane in 80 mL hexadecane and 10 mL toluene in 90 mL hexadecane in 100 mL beakers, respectively. The incubation was carried out at 25 °C for 14 days.

2.7. Evaluation of bacterial growth in crude oil and their degradation efficiency

The growth of bacterial isolates and degradation of crude oil were investigated according to the methods described by Al-Hawash et al. (2018). In total, the six bacterial isolates were grown overnight in nutrient broth and the cells were harvested by centrifugation at 600 rpm for 6 min. The pellets were washed twice with sterile 0.85 % NaCl solution and transferred into F/2 medium. A fixed volume (1 mL equated to 0.01 OD_{600}) of six isolates were individually transferred into separate 250 mL Erlenmeyer flask containing 100 mL F/2 medium followed by the addition of 0.5 mL crude oil. The cultures were incubated in a shaking incubator at 130 rpm at 37 °C for 14 days. The control was prepared similarly except the bacterial inoculum. All experiments were performed in triplicate. The growth of bacteria was assessed by recording the absorbance (or optical density) at 600 nm by UV–visible spectrophotometry after 5, 7, 9, 12 and 14 days.

2.8. Total n-alkanes in control and left n-alkanes in un-degraded crude oil by GC-MS

The procedures described by Al-wasify and Hamed (2016) were modified for GC-MS analysis of crude oil (control) and un-degraded crude oil – i.e. left after inoculation with S1.5 and S2.1 bacterial isolates (7890 A, Agilent Technologies). The GC-MS analysis of crude oil (control) and un-degraded crude oil (residual crude oil) was performed for total n-alkanes (n-C13 to n-C35) in control and left n-alkanes in undegraded crude oil, respectively. The residual crude oil at the end of 14th days of incubation with S1.5 and S2.1 were extracted in chloroform (10 mL×2; 5 mL ×1; total volume 25 mL). The lower organic layer was separated and passed through dried anhydrous sodium sulphate to remove any traces of moisture. The solvent was removed using a rotary evaporator and the oil was isolated. The control and residual oil from the samples (S1.5 and S2.1) were dissolved in 20 mL dichloromethane and transferred into 100 mL Erlenmeyer stoppered flask (Al Kharusi et al., 2016; Viñas et al., 2002). The oil solution was sonicated at 10 ± 1 ℃ for 15 min for thoroughly mixing and dissolving crude oil. This solution was transferred into 25 mL standard volumetric flask and diluted up to mark with dichloromethane. The oil solutions were passed through 0.45 μm polyether sulfone membrane filter and injected into GC-MS auto sampler for detection of n-alkanes (n-C13 to n-C35).

The Perkin Elmer Clarus 600 C MS was coupled with a fused-silica capillary column (Rx_i-5Sil MS column (30 m length × 0.25 mm internal diameter × 0.25 μm film thickness; maximum temperature 350 °C). Helium (ultra-high purity) was used as the carrier gas at a constant flow rate of 1.0 mL min^{-1}. Electron multiplier voltage was auto tuned and the ionizing energy was 70 eV. The transfer line and ion source temperatures were fixed at 280 °C. The injector was set at 290 °C, and the GC oven temperature was programmed from 80°C for 5 min and increased to 280 °C at 10 °C per min for 30 min. The volume of injected sample was 1 μL with a split ratio of 10:1. The mass spectrum was recorded from *m/z* 100–550 amu. The alkanes were identified by matching their retention time and mass spectrum profiles with reference data available in mass spectral library (NIST 2011 v.2.3 and Wiley, 9th edition).

2.9. Molecular docking of n-alkanes with alkane 1-monooxygenase and long-chain alkane monooxygenase

The 3D structures of ligands (C13, C18 and C34) were drawn using Chem3D Pro 12.0 and saved in.sdf format. These.sdf files of ligands were then converted to. mol2 file format using Chimera 1.15 software through structure editing, minimization and Gasteiger charge assignment. The crystallographic structure of 4 proteins namely: Cryo-EM structure of alkane 1-monooxygenase AlkB (PDB code: 8SBB; Organism: *Fontimonas thermophila*), Cryo-EM structure of alkane 1-monooxygenase AlkB-AlkG complex (PDB code: 8F6T; Organism: *Fontimonas thermophila*), crystal structure of long-chain alkane monooxygenase LadA (PDB code: 3B9N, organism: *Geobacillus thermodenitrificans*) and long-chain alkane monooxygenase (LadA) in complex with coenzyme FMN (PDB code: 3B9O, organism: *Geobacillus thermodenitrificans*) were downloaded as a.pdb files from the Protein Data Bank (PDB: https://www.rcsb.org/) and prepared using Chimera 1.15 software. Later, PyRx (0.8) software was used for molecular docking and binding affinity analysis. During the analysis, the grid box was set with the centre coordinates X = 37.8, Y= 80.2862 and Z = 46.2613, and

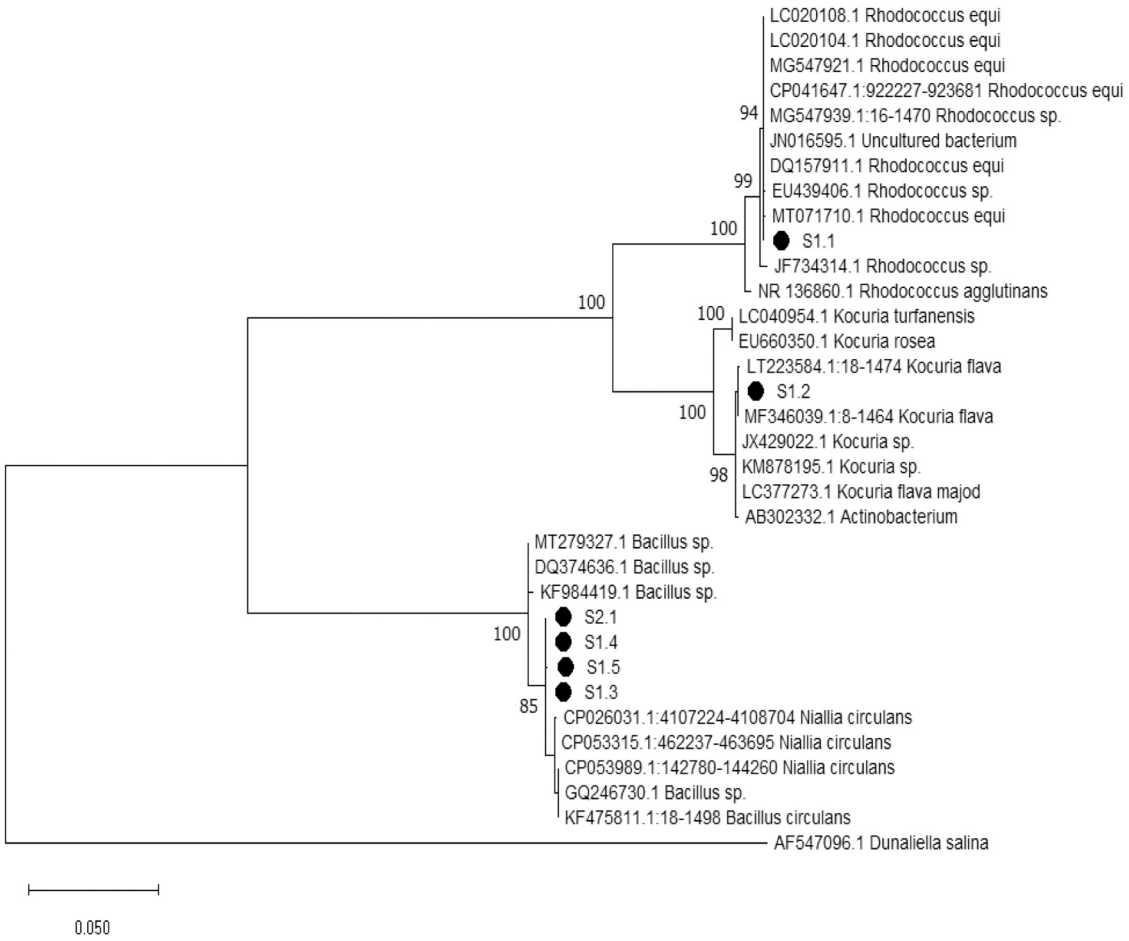

Fig. 1. Maximum likelihood phylogenetic tree showing the relationship between the hydrocarbon degrading bacteria isolates based on 16S rRNA gene sequence. The bootstrap values are based on 1000 replications and the circles represent the bacterial isolates obtained from this study. The bootstrap values less than 70 were not included in the tree. The sequence of 16S rRNA gene from *Dunaliella salina* (AF547096.1) was used as an outgroup. The scale bar represents approximately 0.05 substitutions per nucleotide position. Accession Numbers for the bacterial isolates; PP346386 (S1.1), PP346387 (S1.2), PP346388 (S1.3), PP346389 (S1.4), PP346390 (S1.5) and PP346391 (S2.1).

dimension of 62.2089 Å, 86.9143 Å, and 58.6015 Å for X, Y, and Z, respectively with exhaustiveness 8 to cover the active site residues. During the analysis of all ligands (C13, C18 and C34), the grid box was set with the dimension's coordinates: X = 69.2385 Å, Y= 126.7675 Å and Z = 89.8381 Å for the chain A of 8SBB, X = 53.2159 Å, Y= 98.0885 Å and Z = 94.0964 Å for the chain A of 8F6T; X = 67.4791 Å, Y= 55.7178 Å and Z = 62.1745 Å for the chain B of 3B9N and X = 67.6152 Å, Y= 94.7836 Å and Z = 61.4923 Å for the chain B of 3B9O. The PyMOL (PyMOL2) was used to visualize the 3D diagram showing the overlaid interaction between proteins and the ligands (C13, C18 and C34). Finally, the unified dataset was saved in.pdb format and analysed in Biovia Discovery Studio 2021 to determine the binding interactions, amino acid residues, and bond distances.

2.10. Statistical analysis for significance testing of experimental data

The data collected in the study were statistically analyzed using SigmaPlot (Systat Software Ver. 12.0, San Jose, California USA), IBM SPSS Statistics for windows, version 20.0. Armonk, NY: IBM Corp.), JASP Team (2024) and PAST 4.08. The statistical tests include comparative statistics (t-test and one-way RM-ANOVA), violin plots and Kernel Density estimation (KDE), matrix plots, and raincloud plots. A *p*-value of less than 0.05 was considered statistically significant.

3. Results

3.1. Bacterial isolation and molecular identification

Water samples were procured from two potential sites in Oman and investigated for the isolation of hydrocarbon degrading bacteria. Five bacterial isolates (S1.1, S1.2, S1.3, S1.4 and S1.5) were obtained from location 1 and one bacterial isolate (S2.1) from location 2. The obtained bacterial isolates showed a slight variation in terms of Gram staining and shape as the bacterial isolates were Gram positive with either coccus or bacillus. Based on the preliminary results, four bacterial isolates (S1.3, S1.4, S1.5 and S2.1) were found to be bacilli and phylogenetically belong to the genus *Niallia* based on 16S rRNA gene sequences, as shown in Fig. 1. These isolates shared 99 % sequence similarity to *Niallia circulans* on 16S rRNA gene sequences (previously classified as *Bacillus circulans*) (Gupta et al., 2020). On the other hand, two isolates S1.1 and S1.2 were found to be actinomycetes with > 97 % sequences similarity to *Rhodococcus sp.* and *Kocuria flava,* respectively.

3.2. Bacterial growth and biodegradability of selected hydrocarbons and crude oil

The degradation potential of the bacterial isolates was evaluated by monitoring their growth with (i) hydrocarbons such as n-alkanes (n-hexane and n-octane) and an aromatic hydrocarbon (toluene), and ii) crude oil (a complex mixture of hydrocarbons). The growth of bacterial

Table 1
Bacterial growth on alkanes and aromatic hydrocarbons. The growth on 2 % w/v F/2 agar is indicated as follow: (–) = no growth, (+) =low growth, (++) =medium growth and (+++) = strong growth. The experiment was conducted in triplicates.

Bacterial Isolates	Qualitative Growth		
	n-hexane (C_6H_{14})	n-octane (C_8H_{18})	Toluene (C_6H_5-CH_3)
Control	–	–	–
S1.1	+ +	+ +	+ ++
S1.2	+	+ +	+
S1.3	+	+ +	+ +
S1.4	+ ++	+ +	+ ++
S1.5	+ +	+ ++	+ ++
S2.1	+ ++	+ ++	+ ++

Table 2
The optical density (OD) of bacterial isolates at 600 nm in F/2 liquid medium agar (w/v) with 1 % crude oil v/v at different days.

Days	Control	Bacterial isolates					
		S1.1[a]	S1.2[a]	S1.3[a]	S1.4[a]	S1.5[a]	2.1[b]
	OD at 600 nm						
1	0	0.01	0.01	0.01	0.01	0.01	0.01
5	0	0.39	0.06	0.13	0.26	0.40	0.51
7	0	0.82	0.14	0.35	1.22	1.07	1.00
9	0	0.89	0.62	0.52	1.28	1.64	1.29
12	0	0.89	0.70	0.67	1.39	1.61	1.60
14	0	1.02	0.70	0.70	1.57	1.34	0.88

[a] location1.
[b] location 2.

isolates with n-hexane, n-octane and toluene differed, and hence the degradation pattern would also differ accordingly, as it is evident from Table 1. As such, the growth of S1.5 and S2.1 was found to be more efficient on hexane, octane and toluene, while S1.2 grew better on octane as a simple straight chain with eight carbon atoms and least growth on hexane and toluene. Nevertheless, the best growth was achieved by S1.5 and S2.1 on utilizing n-alkanes and aromatic hydrocarbons.

The bacterial growth of obtained isolates (S1.1, S1.2, S1.3, S1.4 and S1.5) with crude oil (1 %) in F/2 medium was investigated by UV–visible spectrophotometry. As shown in Table 2, the absorbance due to the growth of S1.1, S1.2, S1.3, S1.4, S1.5 and S2.1 in crude oil was increased to 0.39, 0.06, 0.13, 0.26, 0.40 and 0.51 at 600 nm, respectively in 5 days. This significant increase in the absorbance underlined the initial adjustment to the medium and degradation of n-alkanes in crude oil. The maximum absorbance of 1.64 was achieved with S1.5 bacterial isolate in 9 days whereas nearly the same absorbance of 1.60 was achieved in 12 days with 2.1 bacterial isolate. S1.5 bacterial isolate showed the enhanced degradation of n-alkanes when compared with S2.1 bacterial isolate in terms of days.

The isolate S1.5 provided the rapid degradation of n-alkanes present in the crude oil. Further, the decrease in absorbance on 14 days from the saturation point was observed (1.64–1.34 by S1.5 bacterial isolate and 1.60–0.88 by S2.1 bacterial isolate). The early decrease in absorbance from the saturation point justified the breakdown of higher n-alkane to medium n-alkane and finally to least toxic substance i.e. CO_2. Based on the results obtained in terms of absorbance (Table 2), it is evident that the bacterial isolates S1.5 and S2.1 possessed notably higher and faster degradation of n-alkanes in crude oil.

The initial growth rate (υ) of S1.1, S1.2, S1.3, S1.4, S1.5 and S2.1 bacterial isolates was calculated by taking the slope of the initial tangent to the absorbance time curves (1–5 days; Fig. 2) and found to be 4.58×10^{-5} min^{-1}, 7.87×10^{-6} min^{-1}, 1.62×10^{-5} min^{-1}, 3.01×10^{-5} min^{-1}, 4.75×10^{-5} min^{-1} and 5.90×10^{-5} min^{-1}, respectively. The initial growth rate of bacterial isolates based on OD_{600} in decreasing order is as follows: S2.1>S1.5>S1.1>S1.4>S1.3>S1.2. The bacterial isolates S2.1 and S1.5 displayed the highest and second highest initial growth rates, respectively. The order of these isolates was determined from the plot of the logarithm of the initial growth rate (log υ) versus the logarithm of the molar concentration of crude oil (log C) (Fig. 3), and was found to be unity.

The morphological changes of the crude oil with bacterial isolates were also monitored throughout the incubation period in F/2 medium. At the beginning of incubation, crude oil appeared to be floating on F/2 liquid medium. However, as the incubation period progressed to 7 days, the surface of crude oil (control) changed into gelatinous blob followed by decrease in oil viscosity (or surface tension) and increase in the turbidity with emulsification (Fig. 4). The transformation of crude oil

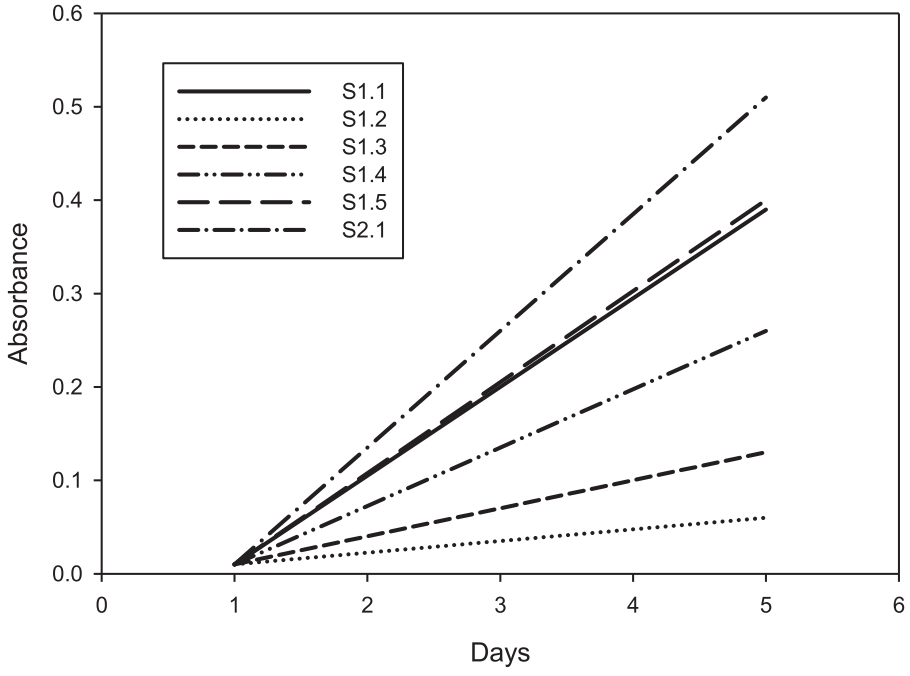

Fig. 2. Absorbance-time curves due to bacterial isolates (S1.1, S1.2, S1.3, S1.4, S1.5 and S2.1) with 0.05 M crude oil in F/2 medium for 5 days.

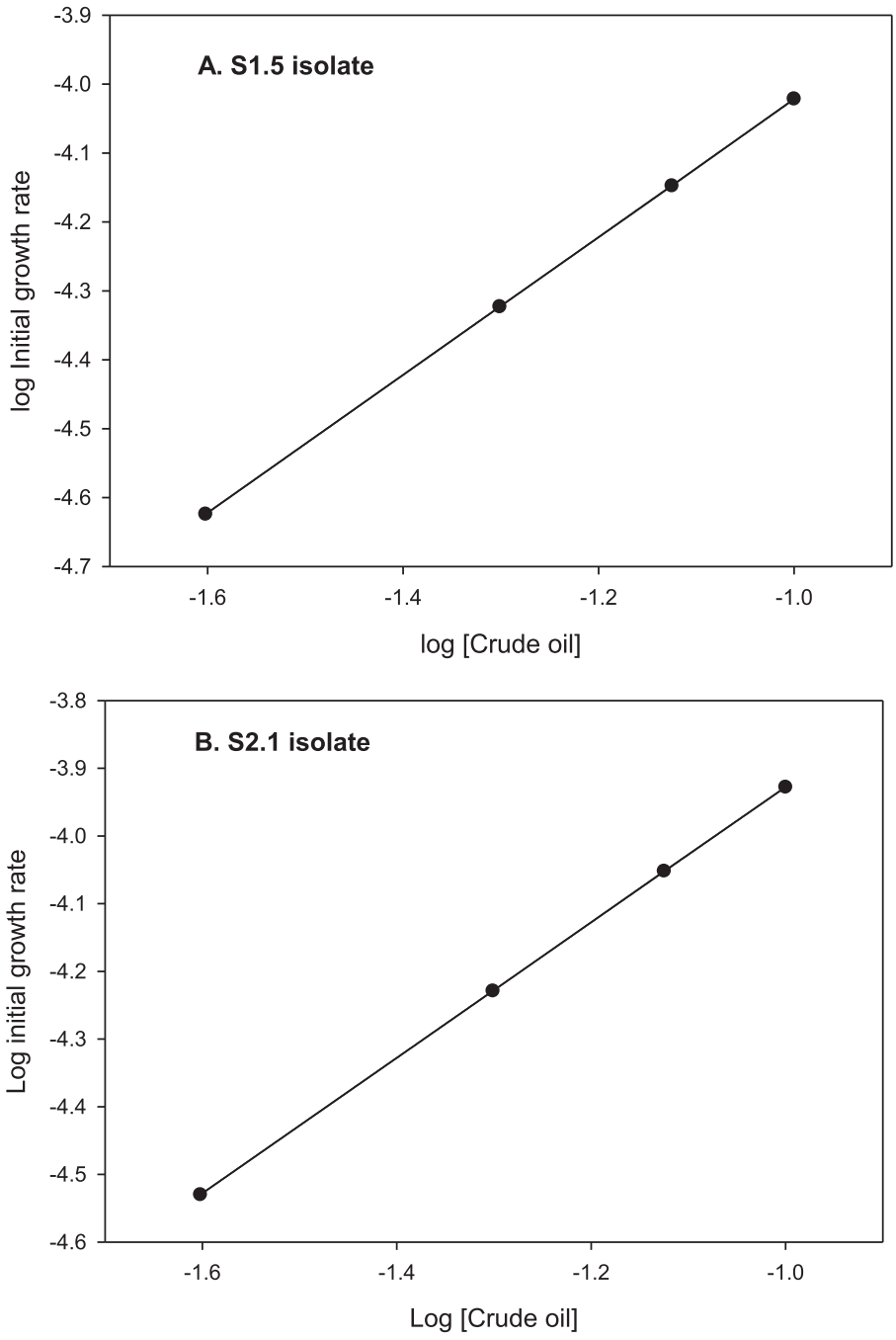

Fig. 3. Log of initial growth rate versus log of molar concentration of crude oil due to (A) S1.5 bacterial isolate and (B) S2.1 bacterial isolate.

into gelatinous form can be considered as pseudo-solubilization because of the possible accumulation of emulsifying agents, hence resulted in the conversion of crude oil into small droplets. This phenomenon supported the spreading of crude oil and formation of emulsion and finally degradation of n-alkanes in crude oil. The morphological changes in crude oil can be seen in Fig. 4 with S.1.5 and S.2.1 bacterial isolates. Hence, these changes pointed towards the ability of bacteria to emulsify and degrade n-alkanes in crude oil.

In addition, a detailed descriptive statistical analysis and one-way ANOVA were performed on the absorbance values given in Table 2. The results revealed that there was a statistically significant difference across all treatments (one-way repeated measures analysis of variance (RM-ANOVA); df= 6; SS= 4.993; MS= 0.832; F= 11.504; $p < 0.001$) (Table 3). The highest mean value ± standard error was obtained with S1.5 bacterial isolate (1.01 ± 0.27) followed by S1.4 and S2.1 bacterial isolates (0.95 ± 0.26 and 0.88 ± 0.23), respectively. However, the maximum absorbance value was recorded for S1.5 (1.640) followed by S2.1 and S1.4 (1.600 and 1.570), respectively. Apart from this, the range values (maximum-minimum) also followed the same pattern i.e. S1.5 >S2.1 >S1.4 (Table 3). It was observed that the isolates, i.e. S1.4, S1.5 and S2.1 exhibited a higher median values and interquartile range (IQR). The degradation potential of obtained bacterial isolates was further tested using the Violin plots (Fig. 5). In addition to this, the Kernel Density Estimation (KDE) exhibited a better unimodal distribution pattern in S1.5 and S2.1, whereas S1.4 exhibited slightly bimodal distribution. Thus, S1.5 and S2.1 are the best bacterial isolates with high degradation levels of n-alkanes in crude oil. Therefore, S1.5 and S2.1 isolates were selected for further studies by GC-MS based on the

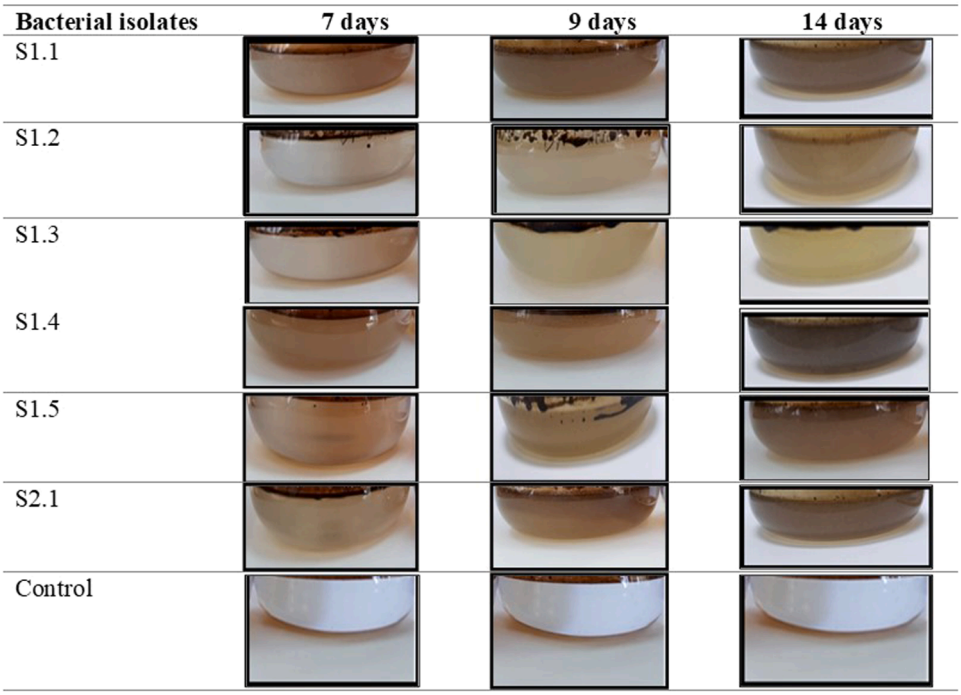

Fig. 4. Morphological changes in crude oil incubated with bacterial isolates in 2 % F/2 medium with 1 % crude oil v/v at different days. Control did not contain bacteria.

Table 3
Descriptive statistics and one-way repeated measure analysis of variance (RM-ANOVA) for the optical density (OD) of bacterial isolates at 600 nm F/2 liquid medium agar (w/v) with 1 % crude oil v/v during the study period of 2 weeks.

Statistics	Control	Bacterial isolates					
		S1.1[a]	S1.2[a]	S1.3[a]	S1.4[a]	S1.5[a]	2.1[b]
	OD at 600 nm						
Median	0	0.820	0.140	0.350	1.250	1.205	0.940
Mean ± SE	0	0.67 ± 0.15	0.37 ± 0.13	0.39 ± 0.11	0.95 ± 0.26	1.01 ± 0.27***	0.88 ± 0.23
IQR	0	0.393	0.600	0.448	0.863	0.975	0.615
Variance	0	0.151	0.112	0.081	0.424	0.448	0.319
Range	0	1.010	0.690	0.690	1.560	1.630	1.590
Minimum	0	0.010	0.010	0.010	0.010	0.010	0.010
Maximum	0	1.020	0.700	0.700	1.570	1.640	1.600

*** $p < 0.001$ (one way RM-ANOVA; df=6; SS=4.993; MS=0.832; F=11.504)
[a] location 1.
[b] loaction 2.

resultant morphological changes in the crude oil, spectrophotometric results pertaining to the bacterial growth and biodegradability supported by comprehensive statistical analysis through ANOVA and Violin plots.

3.3. n-alkanes degradation of crude oil and its analysis by GC-MS

The biodegradation of n-alkanes in crude oil with the most potent bacterial isolates S1.5 and S2.1 were further investigated by GC-MS. The GC-MS chromatograms of n-alkanes for both control and undegraded crude oil after treatment with S1.5 and S2.1 bacterial isolates were recorded and shown in Fig. 6. The detectable n-alkanes in control and undegraded crude oil using GC-MS chromatogram were identified by matching their retention time and mass spectrum profiles with reference data available in mass spectral library. The GC-MS chromatogram of n-alkanes in undegraded crude oils differs from that of control crude oil (GC-MS chromatogram of control crude oil) in terms of peak area of n-alkanes against their respective retention times (C13 to C35). The results of the peak area along with retention times of n-alkanes (C13 to C35) for control and undegraded crude oils are summarized in Table 4.

The percentage degradation of n-alkanes by both bacterial isolates was calculated following the method described in the published paper by Bidja Abena et al. (2019), using the following equation:

$$\% D_{HC} = [(PA_C - PA_I)/ PA_C] \times 100$$

Where $\%D_{HC}$ represents the percentage degradation of n-alkanes in crude oil, PA_C is the peak area of n-alkanes in control crude oil (without bacterial isolates) and PA_I is the peak area of n-alkanes in crude oil inoculated with S1.5 and S2.1 bacterial isolates. The results are shown in Fig. 7.

Table 4 clearly indicated that the percentage degradation of crude oil by the S1.5 bacterial isolate ranged from 64.40 % to 100 %. The decreasing order of n-alkanes degradation by S1.5 was as follows: 100 % (C13) > 98.6 (C16) > 66.81 (C18) > 64.4 (C17). The n-alkanes with carbon numbers C13, C16, C17 and C18 are medium hydrocarbon and appeared to be easily degraded by the S1.5 bacterial isolate.

The percentage degradation of n-alkanes in crude oil by the S2.1 bacterial isolate ranged from 73.91 % to 100 %. The decreasing order n-alkanes degradation by S2.1 was as follows: 100 % (C13, C14, C15 and

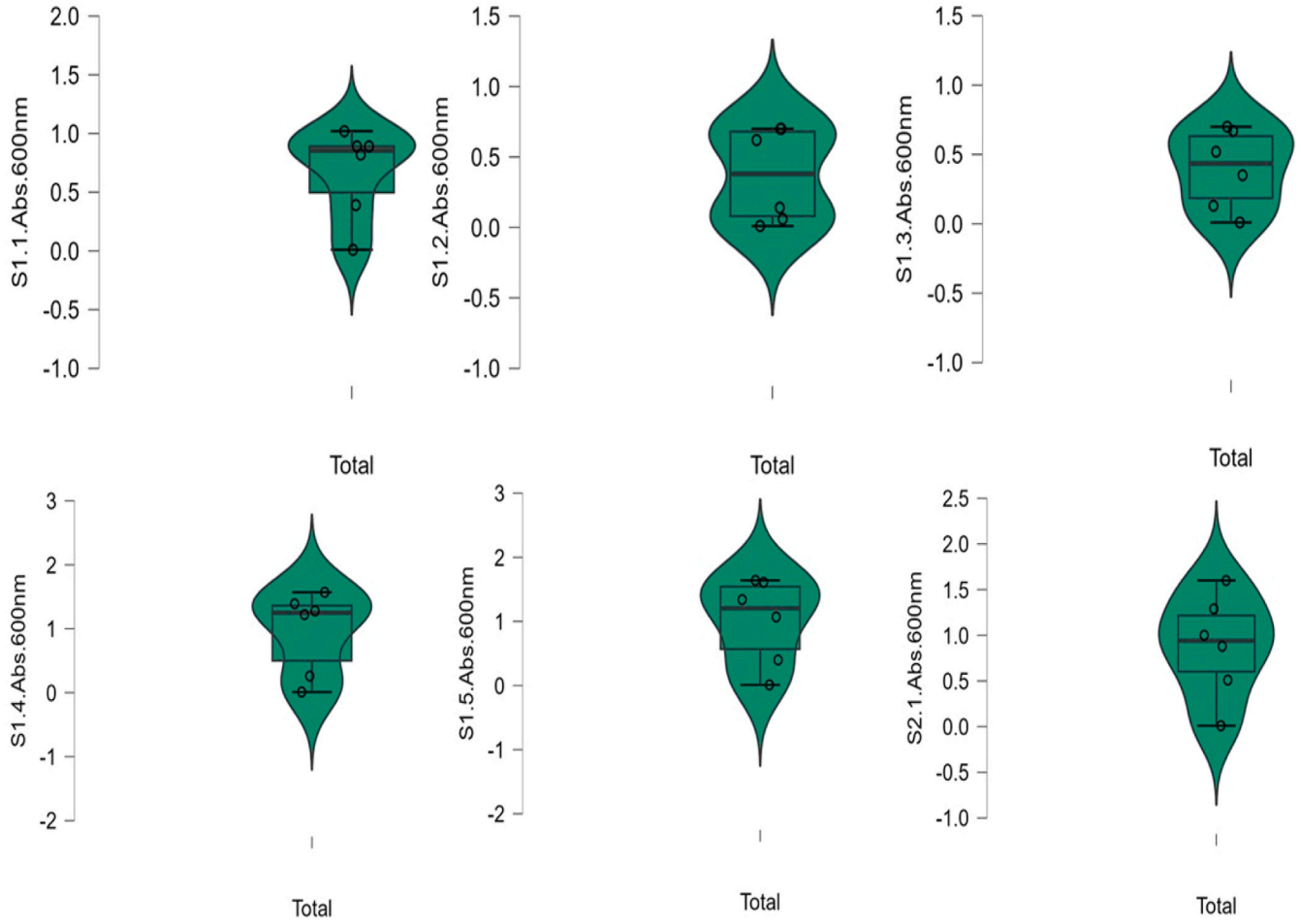

Fig. 5. Violin plots for the absorbance values of bacterial isolates. The last three isolates, i.e. S1.4, S1.5 and S2.1 exhibited a higher interquartile range (IQR). However, the Kernel Density Estimation (KDE) showed that a better unimodal distribution was found in S1.5 and S2.1 isolates only.

C34) > 73.91 (C20). The n-alkanes with carbon numbers C13, C14 and C15 are medium hydrocarbon, while the n-alkanes with carbon numbers C20 and C34 are a higher hydrocarbon. These n-alkanes seem to be easily degraded by S2.1 bacterial isolate. The additional ability of S2.1 to degrade both medium and higher n-alkanes highlighted its importance and significance over the S1.5 bacterial isolate.

The % degradation of n-alkanes (C13 to C35) in crude oil along with retention time with S1.5 and S2.1 bacterial isolates have been visualized using a matrix graph (Fig. 8). The matrix graph clearly revealed the efficiency of S2.1 bacterial isolate over S1.5 bacterial isolate in degrading the medium and higher n-alkanes of crude oil. As can be seen from Fig. 8 that the red shade exhibited higher n-alkanes % degradation of crude oil whereas the orange-yellow represented medium n-alkanes % degradation of crude oil. The further comparative analysis of % degradation efficacies were concluded with raincloud plot and *t*-test analysis (Fig. 9). This finally confirmed that S2.1 bacterial isolate (mean ± SE = 93.613 ± 1.481 %) had a significantly greater n-alkanes degradation (%) (mean difference = 7.537) across all hydrocarbon chains ($t = 3.182$; $p < 0.01$) (two-tailed) than S1.5 bacterial isolate (mean± SE = 86.076 ± 1.847 %).

3.4. Molecular docking of selected n-alkanes with alkane 1-monooxygenase and long-chain alkane monooxygenase

Molecular docking analysis was employed to evaluate the binding characteristics between n-alkanes (C13, C18 and C34 ligands) with alkane 1-monooxygenase (AlkB, chain A of 8SBB; AlkB-AlkG, chain A of 8F6T) and long chain alkane monooxygenase (LadA, chain B of 3B9N; LadA-FMN, chain B of 3B9O). The binding affinities of selected n-alkanes (C13, C18 and C34) with said proteins in the docked complex are summarized in Table 5. It is evident from Table 5 that the binding affinity was varied for n-alkanes (C13, C18 and C34) from −4.5 to −5.5 kcal mol^{-1} for AlkB (8SBB), AlkB-AlkG (8F6T), LadA (3B9N) and LadA-FMN (3B9O). The highest binding affinity of −4.5 kcal mol^{-1}, −5.5 kcal mol^{-1}, −5.3 kcal mol^{-1} and −5.5 kcal mol^{-1} were obtained for C13 with AlkB (8SBB), C13 with AlkB-AlkG (8F6T), C34 with LadA (3B9N) and C34 with LadA-FMN (3B9O), respectively. Hence, it is evidenced that alkane 1-monooxygenase (AlkB and AlkB-AlkG) were effectively degrading medium n-alkane of C13 whereas long chain alkane monooxygenase (LadA and Lad-FMN) degraded higher n-alkane bearing C34. The binding 2D structures of C13 with AlkB (8SBB) and AlkB-AlkG (8F6T) and C34 with LadA (3B9N) and Lad-FMN (3B9O) are shown in Figs. 10 and 11, respectively. The 2D structures (Figs. 10 and 11) were generated by Biovia Discovery Studio, illustrated the interactions, amino acid residues, and bond distances of the selected n-alkanes with the said enzymes. Additionally, the 3D superimposed diagram of C13, C18, and C34 ligands with alkane 1-monooxygenase (AlkB, 8SBB; AlkB-AlkG, 8F6T) and long chain alkane monooxygenase (LadA, 3B9N; Lad-FMN, 3B9O) are shown in Figs. 12 and 13, respectively.

4. Discussion

4.1. Bacterial isolation and molecular identification

A number of hydrocarbons degrading bacteria have been identified in the marine environments with oil pollution. Hydrocarbons are present

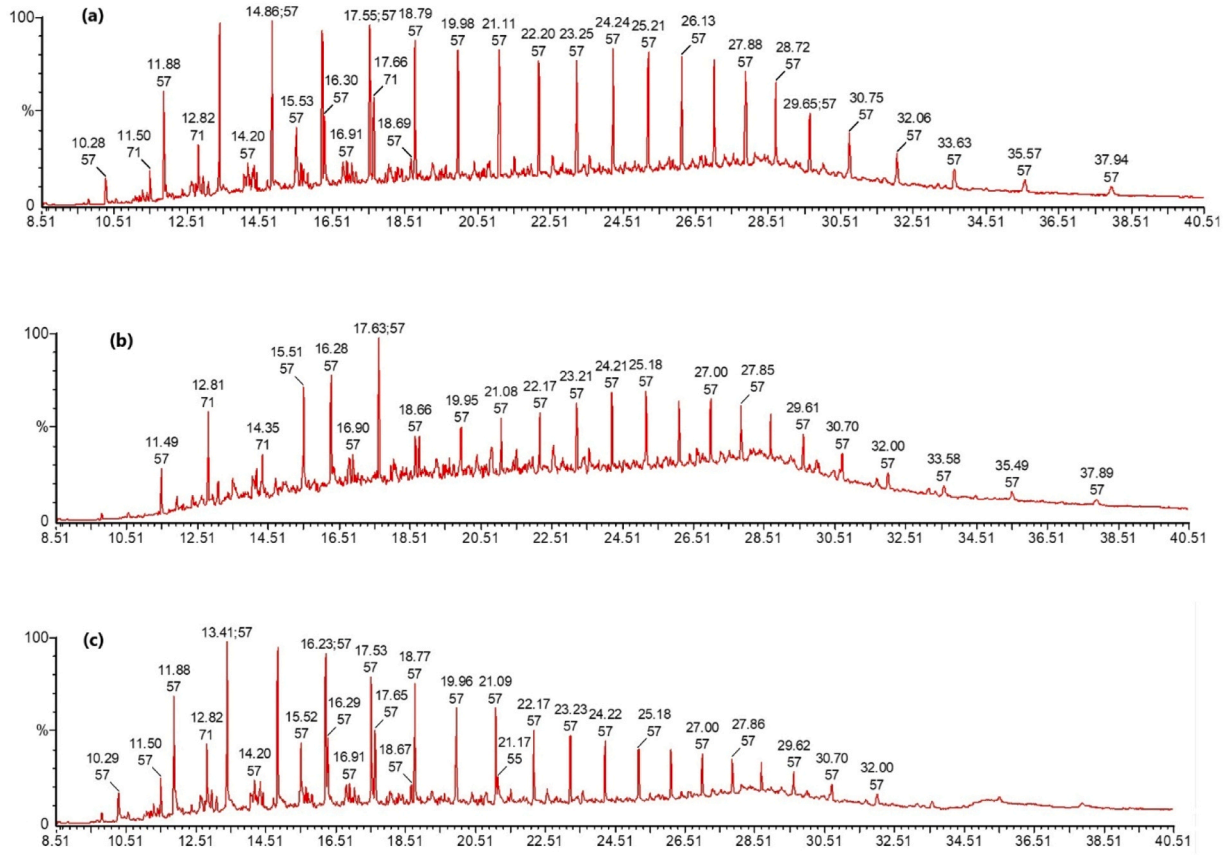

Fig. 6. GC-MS chromaograms for n-alkanes (n-C13 to n-C35) in dichloromethane: (a) control (b) undegraded crude oil (inoculted with S1.5 bacterial isolate) (c) undegraded crude oil (inoculted with S2.1 bacterial isolate).

Table 4
% Degradation of n-alkanes (dissolved in dichloromethane) in crude oils with S1.5. and S2.1 by GC-MS.

Carbon No. of n-alkanes	Retention time (min)	Peak area			% degradation of n-alkanes in crude oils	
		Control	S1.5	S2.1	S1.5	S2.1
C13	10.277	13355774	0	0	100.0	100.0
C14	11.881	70531288	1910369.62	0	97.29	100.0
C15	13.42	130383624	4917255	0	96.23	100.0
C16	14.861	102638424	1438125.125	18741046	98.60	81.74
C17	16.237	86591160	30861790	13441698	64.40	84.48
C18	17.548	87794112	29143142	18663020	66.81	78.74
C19	18.794	85218968	6543976	2587700.25	92.32	96.96
C20	19.975	71703000	7622488	18705486	89.37	73.91
C21	20.95	74103704	1219648	4987994.25	98.35	93.27
C22	22.196	71128568	9462134	5142536	86.70	92.77
C23	23.247	68337752	9902150	2112602	85.51	96.91
C24	24.244	70948936	11467644	2663159	83.84	96.25
C25	25.209	86712672	17584564	6467218	79.72	92.54
C26	26.13	77871200	13256738	4405907	83.00	94.34
C27	27.029	66986644	10363108	2990695	84.53	95.54
C28	27.885	55943512	8229250	2129043	85.29	96.19
C29	28.719	57357164	8231854	1687223	85.65	97.06
C30	29.651	48327376	7139027	1743740	85.23	96.39
C31	30.745	39729384	6428584	949596.7	83.82	97.61
C32	32.056	36426636	5168323	1345426	85.81	96.31
C33	33.628	26259472	4678695	278643	82.18	98.94
C34	35.567	23094008	4250216	0	81.60	100.0
C35	37.94	21833440	3603843	1498588	83.50	93.14

everywhere in the ecosystem, and approximately 800 million tons crude oil are released annually via a combination of natural seeps, accidental releases from the petroleum industry as well as from the cyanobacterial activities (Committee on Oil in the Sea: Inputs, Fates, and E., 2003; Lea-Smith et al., 2015; Love et al., 2021). Hydrocarbons are considered a rich nutritive source for bacteria and have significant environmental implications (Brzeszcz and Kaszycki, 2018; Yakimov et al., 2022; Zhao et al., 2008). In this study, 16S rRNA gene sequences of the bacterial isolates such as S1.3, S1.4, S1.5 and S2.1 were found to be similar to one of a metal resistant and a plant growth promoting strain of *Niallia*

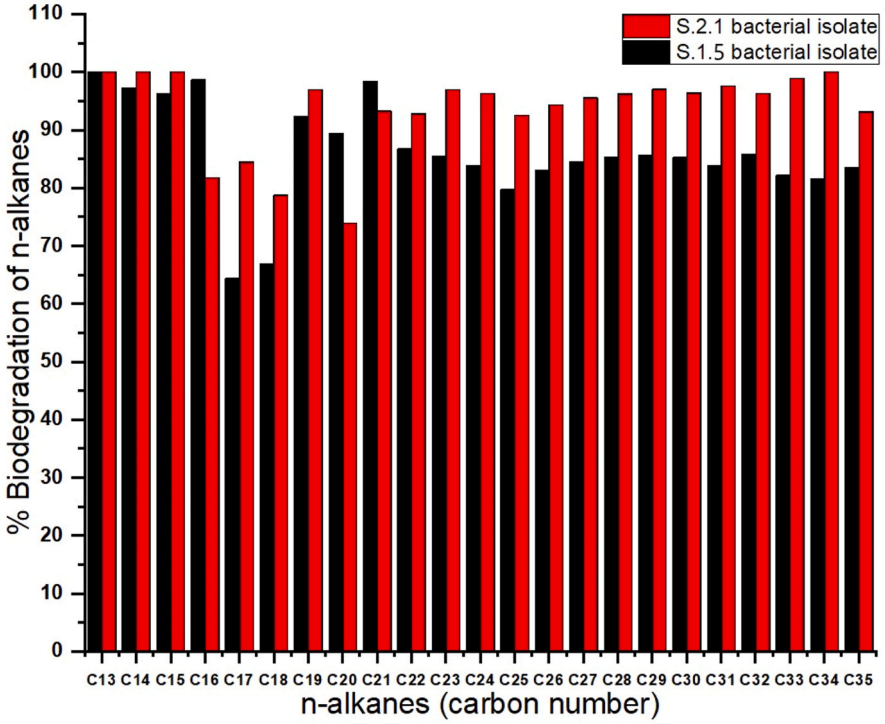

Fig. 7. % Degradation of n-alkanes in crude oil with S1.5 and S2.1 bacterial isolates incubated at 37 °C for 14 days.

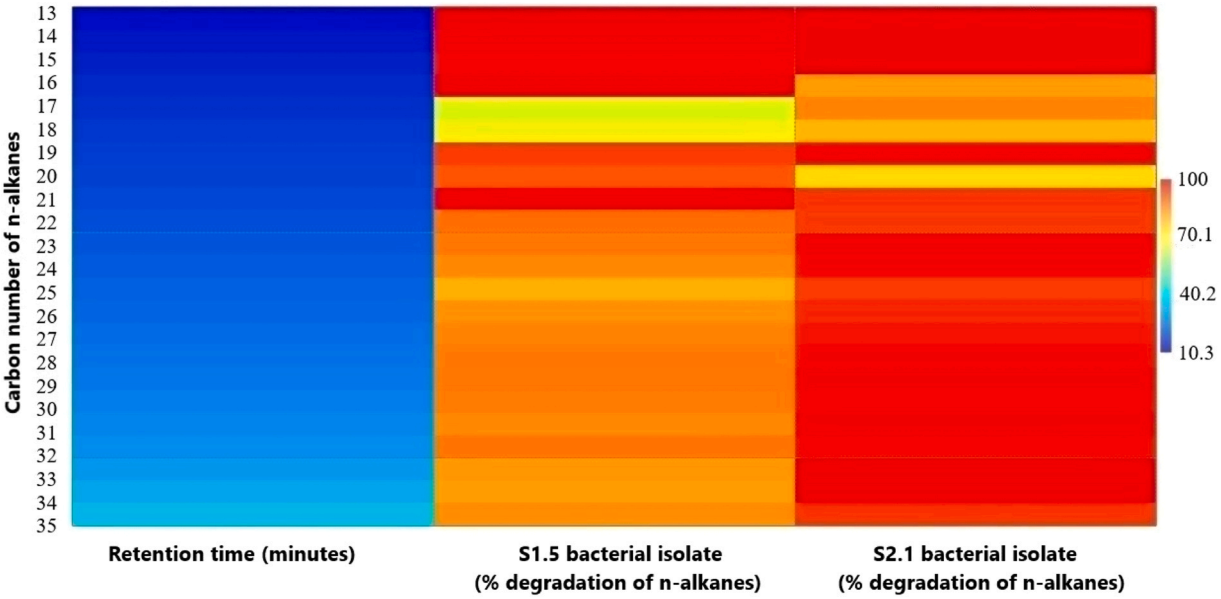

Fig. 8. Matrix plot of retention time (minutes) vs n-alkanes % degradation in crude oil with S1.5 and S2.1 bacterial isolates incubated at 37 °C for 14 days. The color range bar shows the corresponding values of variables. The red color exhibits higher levels, and orange-yellow colors represent lower levels of % degradation. S2.1 isolate effectively degrades the higher n- alkanes than S1.5 isolate.

circulans (Qin et al., 2021; Yilmaz, 2003; Yu et al., 2013). A recent study on the genomic analysis of *Niallia sp*. annotated genes of nitrate reductase, cytochrome P450 and FMN-dependent NADH-azoreductase, indicated potential roles in lignocellulose hydrolysis and bioremediation (Srivastava and Dafale, 2024).

S1.1 and S1.2 bacterial isolates were actinomycetes with sequence similarities of over 97 % to *Rhodococcus sp.* and *Kocuria flava,* respectively. Literature reports the isolation *Rhodococcus sp.* from young volcanic Easter Island in Chile, where it was used to degrade levulinic acid, chloroxylenol and pretilachlor (Xiaoyuan Guo et al., 2023a, 2023b; Liu et al., 2023; Nazari et al., 2022). The genus is known for its resilience in adverse environmental conditions and its ability to bio-remediate oil and oil-bearing products (Xiaoyuan Guo et al., 2023a, 2023b; Ying et al., 2019). The S1.2 isolate, shared sequence identity with *Kocuria flava,* which can grow on various polycyclic aromatic hydrocarbons (Ahmed et al., 2010). Its capability to degrade pyrene and its exposure to high concentrations of polycyclic aromatic hydrocarbons resulted in increased expression of catabolic enzymes such as catechol 2,

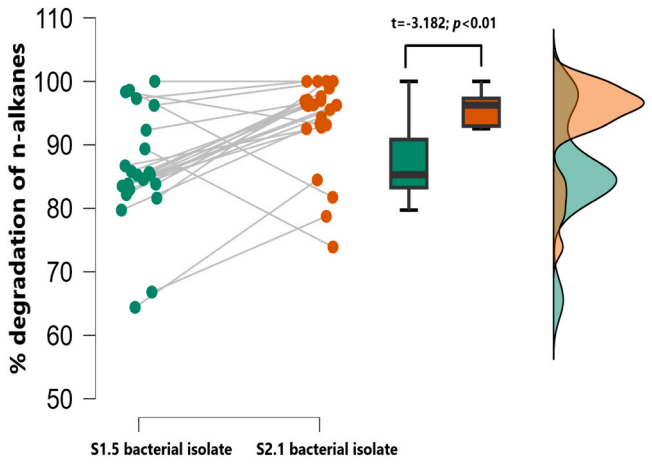

Fig. 9. The raincloud plot showed the comparison and *t*-test between the n-alkanes % degradation efficacies of S 1.5 and S2.1 isolates. Both isolates were effective in their % degradation yet the S1.5 isolate had significantly medium n-alkanes % degradation capabilities than S2.1 isolate (t = -3.182; $p < 0.01$).

Table 5
Binding affinity of C13, C18 and C34 n-alkanes with alkane 1-monooxygenase enzymes (8SBB and 8F6T) and C34 with long-chain alkane monooxygenase enzymes (3B9N and 3B9O).

Species	*Fontimonas thermophila*		*Geobacillus thermodenitrificans*	
Protein	AlkB	AlkB-AlkG	LadA	LadA-FMN
PDB ID	8SBB	8F6T	3B9N	3B9O
Ligands (n-alkanes)	Binding affinity (kcal mol^{-1})			
C13 (tridecane)	−4.5	−5.5	−5.1	−4.7
C18 (octadecane)	−4.4	−4.0	−5.3	−5.1
C34 (tetratriacontane)	−4.4	−4.4	−5.3	−5.5

3-dioxygenase, dehydrogenase, and peroxidase (Sakshi et al., 2021). Additionally, this bacterium has copper-remediating potential, which may also attributed to its oil-degrading nature (Achal et al., 2011).

4.2. Bacterial growth and biodegradability of selected hydrocarbons and crude oil

n-Hexane, n-octane and toluene are among the volatile organic compounds naturally associated with crude oil and are insoluble in water, which justifies their use in monitoring bacterial growth (Bouchard et al., 2008; Mohammadi et al., 2020; Rajabi et al., 2020). In this study, the growth of bacterial isolates (S1.5 and S2.1) was more pronounced with n-hexane, n-octane and toluene compared to other bacterial isolates. The differences in the utilization of individual hydrocarbons by the bacterial isolates highlighted that each bacterium has its own catabolic capacity for the degradative pathway/s.

n-hexane was tentatively degraded by bacteria and entered into degradation through intermediates such as 2-hexanol, 2-hexanone, 5-hexen-2-one, 2,5-hexanedione, 4-methyl-2-pentanone, 3-methyl-1-butanol, 3-methyl-1-butanone and butanal to CO_2 (Lee et al., 2010). n-Octane was degraded via intermediates like 1-octanol, 1-octanal, octanoate, octanoyl-CoA. The end-product formation was based on the degradative pathway followed by the type of bacteria (Wang and Shao, 2013).

The biodegradation of toluene involved both ring cleavage, methylation and hydroxylation. Toluene was reported to be degraded by many isolates of aerobic bacteria utilizing specific monooxygenases. The degradation pathway resulted in the formation of *o*-, *m*-, or *p*-cresol and *m*-cresol may be transformed to 3-methylcatechol or 4-hydroxybenzoate or benzoic acid. Later, benzoic acid may be converted to catechol (Sarsaiya et al., 2017; Shinoda et al., 2004; Zhong et al., 2020).

Crude oil and refinery compounds polluting the water sources may comprise n-alkanes, branched (iso-alkanes) or cycloalkanes (naphthenes) containing up to 60 carbons, and aromatic hydrocarbons (Abrajano et al., 2014). Alkanes are the most abundant hydrocarbons in crude oil, with an estimated abundance of 20–50 % (Rehm and Reiff, 1981). As non-polar molecules with very low chemical activity, alkanes present significant challenges for microbial utilization due to factors such as low water solubility, high degree of accumulation in cell membranes, and higher activation energies (Labinger and Bercaw, 2002; Rojo, 2009). The poor solubility of petroleum hydrocarbons hinders direct contact between cells and petroleum hydrocarbon molecules, limiting degradation opportunities (Liu et al., 2022). Alkane-degrading bacteria typically require specific, induced transport systems to absorb alkanes (Hua et al., 2013). Previous findings indicate that direct uptake of alkane molecules from the water phase is only feasible for low molecular weight alkanes, which are sufficiently soluble to facilitate efficient transport into cells. For medium- and long-chain n-alkanes, microbes may gain access to these compounds by adhering to hydrocarbon droplets (which is facilitated by the hydrophobic cell surface) or by surfactant-facilitated access (Rojo, 2009; Wang et al., 2023).

Various studies suggested that *Bacillus* has the ability to produce natural biosurfactants, which can affect n-alkanes degradation (Das et al., 2024; Wang et al., 2023). Since *Niallia* is a genus previously classified in the Bacillus family, the presence of surfactants can be expected. Surfactants have been reported to increase the uptake and assimilation of n-alkanes in hexadecane (Beal and Betts, 2000; Sabirova et al., 2006). Oil-degrading bacteria typically produce and secrete surfactants of diverse chemical nature, allowing n-alkane emulsification (Lee et al., 2018; Liu et al., 2022). Also, biosurfactants may remain in the extracellular milieu rather than entering the cell (Wang and Shao, 2013).

In this study, it was found that both isolates (S1.5 and S2.1) were capable of degrading medium n-alkanes, but the S2.1 isolate also degraded higher n-alkanes. This may be attributed by any of the afore mentioned factors. The biodegradation process of crude oil resulted in the degradation of n-alkanes, thereby reducing the toxicity of hydrocarbons in environmental samples (Kosaric, 2001). The significance of n-alkane degradation in crude oil by S1.5 and S2.1 isolates was statistically proven using descriptive statistical analysis and one-way ANOVA. The n-alkane degradation was significant, with a p-value of less than 0.05 and an F-value of 11.504. Violin plots supported the degradation pattern of n-alkanes by S1.5 and S2.1, showing a unimodal distribution pattern for both isolates i.e. S1.5 and S2.1.

4.3. n-alkanes degradation of crude oil and its analysis by GC-MS

n-alkanes (C_nH_{2n+2}) mostly available in crude oil are C13 (tridecane), C14 (tetradecane), Cl5 (pentadecane), C16 (hexadecane), Cl7 (heptadecane), Cl8 (octadecane), C19 (nonadecane), C20 (eicosane), C21 (henicosane), C22 (docasane), C23 (tricosane), C24 (Tetracosane), C25 (Pentacosane), C26 (Hexacosane), C27 (Heptacosane), C28 (Octacosane), C29 (Nonacosane), C30 (Triacontane), C31 (Hentriacontane, C32 (Dotriacontane), C33 (Tritriacontane), C34 (Tetratriacontane) and C35 (Pentatriacontane). S2.1 bacterial isolate was found to be an efficient degrader for the medium (C13, C14, C15) and higher n-alkanes (C34) % degradation (73.91–100 %) of crude oil over medium n-alkane (C13, C16, C17, C18) % degradation (64.40–100 %) of crude oil with S1.5 bacterial isolate in a time period of 14 days. 100 % degradation of n-alkanes was achieved for n-alkanes constituting C13 with S1.5 bacterial isolate and C13, C14, C15 and C34 with S2.1 bacterial isolate. The same 100 % degradation of C20 was reported with *Pseudomonas frederiksbergensis* in 25 days (Abdel-Mageed et al., 2013).

Several regulators and multiple enzymes have been reported to control the utilization of n-alkanes in different bacteria. Additionally, various transcriptional regulators and diverse transcription modes likely

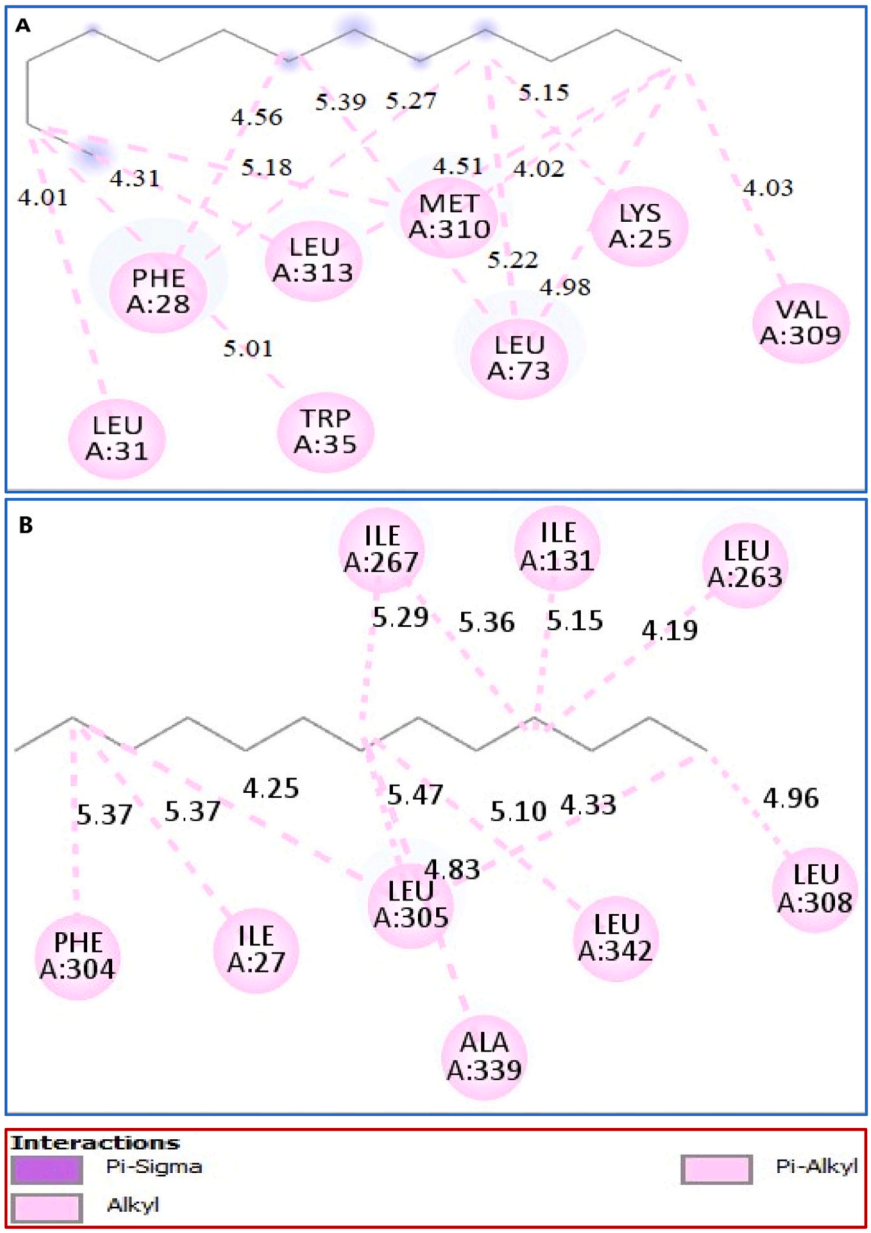

Fig. 10. 2D molecular docked structures of alkane 1-monooxygenase enzymes: (A) C13 with AlkB (8SBB) & (B) C13 with AlkB-AlkG (8F6T).

exist in different microbes. Microbes respond to and utilize *n*-alkanes by altering their cellular regulatory network and initiating the transcription of related hydroxylase genes (Ji et al., 2019; Liu et al., 2014). These factors may explain the lower degradation percentage of C17 and C18 by S1.5 and C20 by S2.1.

4.4. *Molecular docking of selected n-alkanes with selected proteins*

In this study, n-alkanes: C13-C15 and C34 in the crude oil were completely degraded by S2.1, whereas the bacterial isolate achieved the complete degradation of C13. The docking results (2D and 3D structures) showed that n-alkane bearing C13 exhibited strong binding with alkane 1-monooxygenase enzymes (8SBB and 8F6T) and C34 with long-chain alkane monooxygenase enzymes (3B9N and 3B9O) forming bonds that included alkyl, pi-alkyl interactions, and van der Waals forces, based on similar compatibility principles. Another study corroborated these findings, suggesting that the immobilized carrier established a strong hydrophobic connection with the n-alkanes in crude oil, ultimately facilitating the subsequent biodegradation of the crude oil (Fu et al., 2021). In addition to this, the degradation of n-alkanes by a particular type of alkane hydroxylase is based on the chain length of the n-alkane substrate. For example, an integral membrane non-heme iron monooxygenase enzyme e.g. AlkB catalyzes the initial hydroxylation of mid-chain n-alkanes (C8-C16), while a long-chain alkane monooxygenase enzymes such as LadA initiates the hydroxylation of the long-chain n-alkanes (>C18) (Moreno and Rojo, 2010; Nie et al., 2013). The docking with crystal structure of long-chain alkane monooxygenase enzymes as LadA included as the apoenzyme (3B9N) and, its complex with the mononucleotide coenzyme FMN (3B9O) from *Geobacillus thermodenitrificans* as a member of Bacillaceae family as *Niallia circulans* (Feng et al., 2007; Li et al., 2008). Since no crystal structure is currently available for alkane 1-monooxygenase enzyme form Bacillaceae family, the crystal structure of alkane 1-monooxygenase (PDB: 8SBB) and alkane 1-monooxygenase AlkB-AlkG complex (PDB: 8F6T) were taken from *Fontimonas thermophila* (Xue Guo et al., 2023a, 2023b). However, homologs of alkane monooxygenase (AlkB) have been detected at the transcript levels in the member of Bacillaceae family during n-alkanes degradation (Korshunova et al., 2011). Additionally, a comprehensive

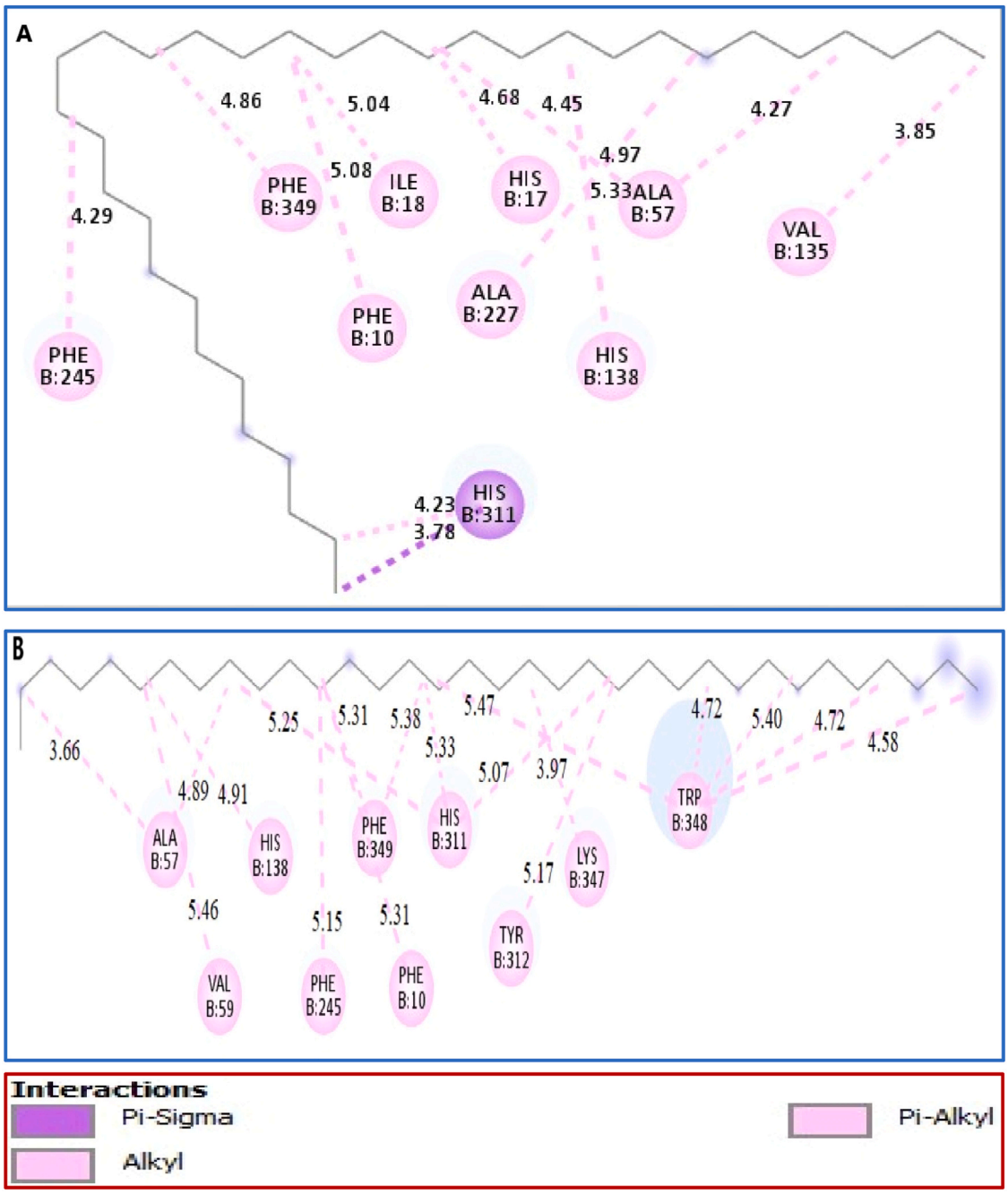

Fig. 11. 2D molecular docked structures of long chain alkane monooxygenase enzymes: (A) C34 with LadA (3B9N) & (B) C34 with Lad-FMN (3B9O).

genomic survey highlighted the presence of AlkB gene alongside AlkG in over 390,000 isolates spanning 3687 genera thereby emphasizing on considering AlkB gene as a molecular marker for n-alkanes degradation (Christian et al., 2020; Wang et al., 2022).

The highest binding affinity of −4.5 and −5.5 kcal mol^{-1} for C13 with mid-chain n-alkanes (C8-C16) degraders such as AlkB (8SBB) and AlkB-AlkG (8F6T) were justified and parallel to our experimental findings of 100 % degradation of n-alkane bearing C13. Similarly, the highest binding affinity of −5.3 and −5.5 kcal mol^{-1} for C34 with long-chain n-alkanes (>C18) degraders (LadA, 3B9N and LadA-FMN, 3B9O) were justified too and parallel to our experimental findings of 100 % degradation of C34 n-alkane. As per the reported literature (Das et al., 2024), the n-alkane degradation pathway was initiated with the oxidation of n-alkane via hydroxylation of a terminal methyl group to alcohols then to corresponding aldehydes and fatty acids. The fatty acids were then conjugated to CoA to generate acetyl-CoA via β-oxidation.

4.5. Statistical analysis

The percentage degradation of n-alkanes in crude oil by S1.5 and S2.1 was visualized using matrix graph, revealing higher degradation efficiency for S2.1. The significance of degradation was tested using a Raincloud plot and *t*-test, which supported the higher percentage degradation by S2.1 (mean ± SE = 93.613 ± 1.481 %) compared to S1.5 (mean ± SE = 86.076 ± 1.847 %). The degradation of *n*-alkanes in crude oil was significant, as indicated by the lower p-value (less than 0.05) and lesser t-value (t = -3.182) when compared with the tabulated t-value.

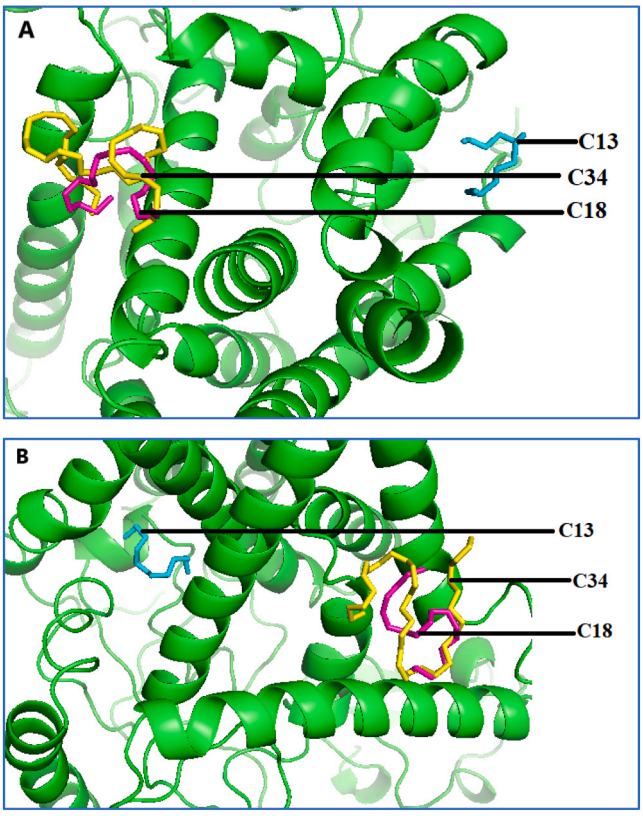

Fig. 12. 3D superimposed diagram of n-alkanes (C13, C18 and C34) with alkane monooxygenase enzymes on chain A of (A) 8SBB and (B) 8F6T.

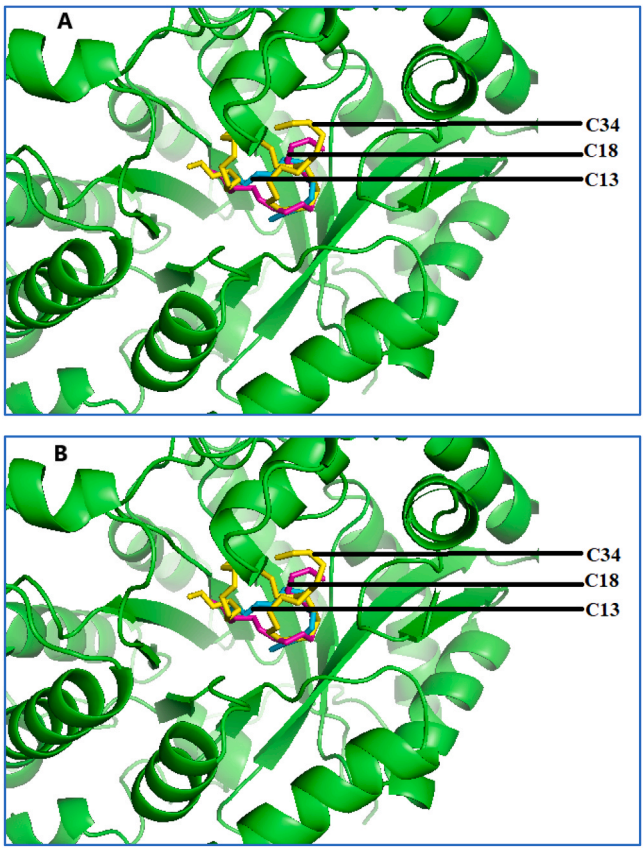

Fig. 13. 3D superimposed diagram of n-alkanes (C13, C18 and C34) with long chain alkane monooxygenase enzymes on chain B of (A) 3B9N and (B) 3B9O.

5. Conclusions

Contamination of marine ecosystem by petroleum products is a pressing issue. Bacterial mediated degradation of n-alkanes in crude oil by marine bacterial isolates holds enormous potential for future applications in the remediation of petroleum-contaminated marine environments. Hydrocarbon scavenging bacteria, adapted to harsh marine conditions, showcase a significant ability to break down complex hydrocarbons found in crude oil. The present study explored the isolation, identification and characterization of potential marine bacterial isolates capable of degrading n-alkanes in crude oil. The results of this study report the isolation of six hydrocarbon-degrading bacteria belonging to *Rhodococcus*, *Kocuria*, and *Niallia* genera based on their 16S rRNA gene analysis. Among these, two *Niallia* isolates exhibited promising degradative capabilities for n-alkanes in crude oil. The *Niallia* isolate S2.1 efficiently degraded both medium and higher n-alkanes in crude oil as: 100 % degradation of C13, C14, C15 and C34, and 73.91 % degradation (C20). While the *Niallia* isolate S1.5 showed a promising ability to degrade medium n-alkanes as: (100 % degradation of C13; 98.6 % degradation of C16, 66.81 % degradation of C18, and 64.4 % degradation of C17. The findings indicated that the bacterial isolate S2.1 can individually degrade both medium and higher n-alkanes, whereas the bacterial isolate S1.5 is more effective with medium n-alkanes. This is further supported by molecular docking studies for the selected n-alkanes (C13, C18 and C34) with alkane 1-monooxygenase enzymes (8SBB and 8F6T) and long-chain alkane monooxygenase enzymes (3B9N and 3B9O) suggesting the potential of exploiting S1.5 and S2.1 isolates as effective agents for future bioremediation applications.

CRediT authorship contribution statement

Ahmed Qamar Uddin: Visualization. **Mia Md. Abdur Rashid:** Visualization. **Al Hoqani Umaima Hamed:** Writing – review & editing, Writing – original draft, Visualization, Supervision, Resources, Methodology, Funding acquisition, Conceptualization. **Sah Pankaj:** Writing – review & editing, Writing – original draft, Visualization, Validation, Formal analysis. **Al Harthi Jokha Salim:** Validation, Methodology, Investigation. **Bani Saad Zainab Nasser:** Validation, Methodology, Investigation. **Al Nabhani Zainab Saif:** Validation, Methodology, Investigation. **Fnais Mohammed S.:** Writing – review & editing, Funding acquisition. **Azmi Syed Najmul Hejaz:** Writing – review & editing, Writing – original draft, Visualization, Methodology, Data curation. **Vavolil P Jayachandran:** Writing – review & editing, Writing – original draft. **Al Habsi Huda Sultan:** Supervision, Project administration, Investigation. **Reddy Salla Hemadri:** Writing – review & editing, Writing – original draft. **Abdelrahman Kamal:** Writing – review & editing, Funding acquisition.

Declaration of Competing Interest

The authors declare that they have no known competing financial interests or personal relationships that could have appeared to influence the work reported in this paper.

Acknowledgments

The authors are grateful to the University of Technology and Applied Sciences Muscat for providing the required facilities and support for the conduct of the research project. This research project is funded by the Ministry of Higher Education, Research and Innovation, Sultanate of Oman under Block Funding Program with agreement No. TRC/BFP/HCT/01/2019. The UHH thanks Dr. Sajjad Asaf and Dr. Mohammed Mahboob for their guidance and support in processing the DNA sequence and construct the phylogenetic tree. In addition to this, all

authors extend their deep thanks and gratitude to the Researchers Supporting Project Number (RSP2025R351), King Saud University, Riyadh, Saudi Arabia for funding this research article.

Data Availability

Data will be made available on request.

References

Abed, R.M.M., Zein, B., Al-Thukair, A., de Beer, D., 2007. Phylogenetic diversity and activity of aerobic heterotrophic bacteria from a hypersaline oil-polluted microbial mat. Syst. Appl. Microbiol 30, 319–330. https://doi.org/10.1016/j.syapm.2006.09.001.

Abrajano, T.A., Yan, B., O'Malley, V., 2014. High molecular weight petrogenic and pyrogenic hydrocarbons in aquatic environments. Treatise Geochem. Second Ed. 11, 481–509. https://doi.org/10.1016/B978-0-08-095975-7.00913-X.

Achal, V., Pan, X., Zhang, D., 2011. Remediation of copper-contaminated soil by Kocuria flava CR1, based on microbially induced calcite precipitation. Ecol. Eng. 37, 1601–1605. https://doi.org/10.1016/J.ECOLENG.2011.06.008.

Agunbiade, M., Oladipo, B., Ademakinwa, A.N., Awolusi, O., Adesiyan, I.M., Oyekola, O., Ololade, O., Ojo, A., 2022. Bioflocculant produced by Bacillus velezensis and its potential application in brewery wastewater treatment. Sci. Rep. 12, 1–12. https://doi.org/10.1038/s41598-022-15193-8.

Ahmed, R.Z., Ahmed, R.Z., Ahmed, N., Gadd, G.M., 2010. Isolation of two Kocuria species capable to growing on various polycyclic aromatic hydrocarbons. Isolation of two Kocuria species capable of growing on various polycyclic aromatic hydrocarbons. Artic. Afr. J. Biotechnol. 9, 3611–3617. https://doi.org/10.5897/AJB2010.000-3224.

Al Kharusi, S., Abed, R.M.M., Dobretsov, S., 2016. EDTA addition enhances bacterial respiration activities and hydrocarbon degradation in bioaugmented and non-bioaugmented oil-contaminated desert soils. Chemosphere 147, 279–286. https://doi.org/10.1016/j.chemosphere.2015.12.114.

Al-Hawash, A.B., Alkooranee, J.T., Abbood, H.A., Zhang, J., Sun, J., Zhang, X., Ma, F., 2018. Isolation and characterization of two crude oil-degrading fungi strains from Rumaila oil field, Iraq. Biotechnol. Rep. 17, 104–109. https://doi.org/10.1016/j.btre.2017.12.006.

Al-wasify, R.S., Hamed, S.R., 2016. Bacterial biodegradation of crude oil using local isolates, 1–1 Int. J. Bacteriol. 2016. https://doi.org/10.1155/2016/6013871.

Atlas, R.M., 1995. Bioremediation of petroleum pollutants. Int. Biodeterior. Biodegrad. 35, 317–327. https://doi.org/10.1016/0964-8305(95)00030-9.

Beal, R., Betts, W.B., 2000. Role of rhamnolipid biosurfactants in the uptake and mineralization of hexadecane in Pseudomonas aeruginosa. J. Appl. Microbiol 89, 158–168. https://doi.org/10.1046/j.1365-2672.2000.01104.x.

Bidja Abena, M.T., Sodbaatar, N., Li, T., Damdinsuren, N., Choidash, B., Zhong, W., 2019. Crude oil biodegradation by newly isolated bacterial strains and their consortium under soil microcosm experiment. Appl. Biochem. Biotechnol. 189, 1223–1244. https://doi.org/10.1007/s12010-019-03058-2.

Bouchard, D., Höhener, P., Hunkeler, D., 2008. Carbon isotope fractionation during volatilization of petroleum hydrocarbons and diffusion across a porous medium: a column experiment. Environ. Sci. Technol. 42, 7801–7806. https://doi.org/10.1021/es800391s.

Brzeszcz, J., Kaszycki, P., 2018. Aerobic bacteria degrading both n-alkanes and aromatic hydrocarbons: an undervalued strategy for metabolic diversity and flexibility. Biodegradation 29, 359–407. https://doi.org/10.1007/s10532-018-9837-x.

Christian, W.C., Butler, T.M., Ghannam, R.B., Webb, P.N., Techtmann, S.M., 2020. Phylogeny and diversity of alkane-degrading enzyme gene variants in the Laurentian great lakes and Western atlantic. FEMS Microbiol. Lett. 367, 1–9. https://doi.org/10.1093/femsle/fnaa182.

Committee on Oil in the Sea: Inputs, Fates, and E, 2003. Oil in the Sea III: Inputs, Fates, and Effects. National Academies Press, Washington (DC), United State (US). https://doi.org/10.17226/10388.

Das, A., Das, N., Rajkumari, J., Pandey, P., Pandey, P., 2024. Exploring the bioremediation potential of Bacillus spp. for sustainable mitigation of hydrocarbon contaminants. Environ. Sustain 7, 135–156. https://doi.org/10.1007/s42398-024-00309-9.

Dealtry, S., Ding, G.C., Weichelt, V., Dunon, V., Schlüter, A., Martini, M.C., Papa, M.F., Lagares, Del, Amos, A., Wellington, G.C.A., Gaze, E.M.H., Sipkema, W.H., Sjöling, D., Springael, S., Heuer, D., Elsas, H., Van, J.D., Thomas, C., Smalla, K., 2014. Cultivation-independent screening revealed hot spots of IncP-1, IncP-7 and IncP-9 plasmid occurrence in different environmental habitats. PLoS One 9. https://doi.org/10.1371/journal.pone.0089922.

Feng, L., Wang, W., Cheng, J., Ren, Y., Zhao, G., Gao, C., Tang, Y., Liu, X., Han, W., Peng, X., Liu, R., Wang, L., 2007. Genome and proteome of long-chain alkane degrading Geobacillus thermodenitrificans NG80-2 isolated from a deep-subsurface oil reservoir. Proc. Natl. Acad. Sci. U. S. A. 104, 5602–5607. https://doi.org/10.1073/pnas.0609650104.

Fu, X.G., Shi, K., Xue, J.L., Chen, C., Bai, Y., Qiao, Y.L., Liu, Y.X., Hu, X.M., Gao, Y., Yu, H., 2021. Systematic adsorption process of petroleum hydrocarbon by immobilised petroleum-degradation bacteria system in degradation pathways. Pet. Sci. 18, 1543–1550. https://doi.org/10.1016/j.petsci.2021.09.009.

Guillard, R.R.L., Hargraves, P.E., 1993. Stichochrysis immobilis is a diatom, not a chrysophyte. Phycologia 32, 234–236. https://doi.org/10.2216/i0031-8884-32-3-234.1.

Guo, X., Zhang, J., Han, L., Lee, J., Williams, S.C., Forsberg, A., Xu, Y., Austin, R.N., Feng, L., 2023b. Structure and mechanism of the alkane-oxidizing enzyme AlkB. Nat. Commun. 14. https://doi.org/10.1038/s41467-023-37869-z.

Guo, X., Qiu, L., Liang, Z., Lu, Q., Wang, S., Shim, H., 2023a. Isolation and characterization of Rhodococcus sp. GG1 for metabolic degradation of chloroxylenol. Chemosphere 338. https://doi.org/10.1016/j.chemosphere.2023.139462.

Gupta, R.S., Patel, S., Saini, N., Chen, S., 2020. Robust demarcation of 17 distinct bacillus species clades, proposed as novel bacillaceae genera, by phylogenomics and comparative genomic analyses: Description of robertmurraya kyonggiensis sp. nov. and proposal for an emended genus bacillus limiting it o. Int. J. Syst. Evol. Microbiol 70, 5753–5798. https://doi.org/10.1099/ijsem.0.004475.

Hua, F., Wang, H.Q., Li, Y., Zhao, Y.C., 2013. Trans-membrane transport of n-octadecane by Pseudomonas sp. DG17. J. Microbiol 51, 791–799. https://doi.org/10.1007/s12275-013-3259-6.

ITOPF, 2024. Oil Tanker Spill Statistics 2023 [WWW Document]. URL ⟨https://www.itopf.org/news-events/news/oil-tanker-spill-statistics-2023/⟩ (accessed 2.6.24).

Ji, N., Wang, X., Yin, C., Peng, W., Liang, R., 2019. CrgA protein represses AlkB2 monooxygenase and regulates the degradation of medium-to-long-chain n-alkanes in pseudomonas aeruginosa SJTD-1. Front. Microbiol 10, 1–15. https://doi.org/10.3389/fmicb.2019.00400.

Korshunova, A.V., Tourova, T.P., Shestakova, N.M., Mikhailova, E.M., Poltaraus, A.B., Nazina, T.N., 2011. Detection and transcription of n-alkane biodegradation genes (alkB) in the genome of a hydrocarbon-oxidizing bacterium Geobacillus subterraneus K. Microbiology 80, 682–691. https://doi.org/10.1134/S0026261711050079.

Kosaric, N., 2001. Biosurfactants and their application for soil bioremediation. Food Technol. Biotechnol. 39, 259–304.

Kothari, V., 1963. Microbial degradation of hydrocarbons. Prog. Ind. Microbiol 19, 1–33.

Labinger, J.A., Bercaw, J.E., 2002. Understanding and exploiting C–H bond activation. Nature 417, 507–514. https://doi.org/10.1038/417507a.

Lea-Smith, D.J., Biller, S.J., Davey, M.P., Cotton, C.A.R., Sepulveda, B.M.P., Turchyn, A.V., Scanlan, D.J., Smith, A.G., Chisholm, S.W., Howe, C.J., 2015. Contribution of cyanobacterial alkane production to the ocean hydrocarbon cycle. Proc. Natl. Acad. Sci. U. S. A. 112, 13591–13596. https://doi.org/10.1073/pnas.1507274112.

Lee, D.W., Lee, H., Kwon, B.O., Khim, J.S., Yim, U.H., Kim, B.S., Kim, J.J., 2018. Biosurfactant-assisted bioremediation of crude oil by indigenous bacteria isolated from Taean beach sediment. Environ. Pollut. 241, 254–264. https://doi.org/10.1016/j.envpol.2018.05.070.

Lee, E.H., Kim, J., Cho, K.S., Ahn, Y.G., Hwang, G.S., 2010. Degradation of hexane and other recalcitrant hydrocarbons by a novel isolate, Rhodococcus sp. EH831. Environ. Sci. Pollut. Res. 17, 64–77. https://doi.org/10.1007/s11356-009-0238-x.

Li, L., Liu, X., Yang, W., Xu, F., Wang, W., Feng, L., Bartlam, M., Wang, L., Rao, Z., 2008. Crystal structure of long-chain alkane monooxygenase (LadA) in complex with coenzyme FMN: unveiling the long-chain alkane hydroxylase. J. Mol. Biol. 376, 453–465. https://doi.org/10.1016/j.jmb.2007.11.069.

Liu, H., Xu, J., Liang, R., Liu, J., 2014. Characterization of the medium- And long-chain n-alkanes degrading pseudomonas aeruginosa strain SJTD-1 and its alkane hydroxylase genes. PLoS One 9. https://doi.org/10.1371/journal.pone.0105506.

Liu, H., Liu, S., Liu, H., Liu, M., Yin, X., Lu, P., Hong, Q., Liu, A., Wan, R., Fang, S., 2023. Revealing the driving synergistic degradation mechanism of Rhodococcus sp. B2 on the bioremediation of pretilachlor-contaminated soil. Sci. Total Environ. 856. https://doi.org/10.1016/j.scitotenv.2022.159086.

Liu, Y., Wu, J., Liu, Y., Wu, X., 2022. Biological process of alkane degradation by gordonia sihwaniensis. ACS Omega 7, 55–63. https://doi.org/10.1021/acsomega.1c01708.

Love, C.R., Arrington, E.C., Gosselin, K.M., Reddy, C.M., Van Mooy, B.A.S., Nelson, R.K., Valentine, D.L., 2021. Microbial production and consumption of hydrocarbons in the global ocean. Nat. Microbiol 6, 489–498. https://doi.org/10.1038/s41564-020-00859-8.

Mohammadi, L., Rahdar, A., Bazrafshan, E., Dahmardeh, H., Susan, M.A.B.H., Kyzas, G. Z., 2020. Petroleum hydrocarbon removal fromwastewaters: A review. Processes. https://doi.org/10.3390/PR8040447.

Moreno, R., Rojo, F., 2010. Enzymes for Aerobic Degradation of Alkanes. Handbook of Hydrocarbon and Lipid Microbiology. Springer. https://doi.org/10.1007/978-3-540-77587-4_59.

Nazari, M.T., Simon, V., Machado, B.S., Crestani, L., Marchezi, G., Concolato, G., Ferrari, V., Colla, L.M., Piccin, J.S., 2022. Rhodococcus: a promising genus of actinomycetes for the bioremediation of organic and inorganic contaminants. J. Environ. Manag. https://doi.org/10.1016/j.jenvman.2022.116220.

Nie, Y., Fang, H., Li, Y., Chi, C.Q., Tang, Y.Q., Wu, X.L., 2013. The genome of the moderate halophile amycolicicoccus subflavus DQS3-9A1T reveals four alkane hydroxylation systems and provides some clues on the genetic basis for its adaptation to a petroleum environment. PLoS One 8. https://doi.org/10.1371/journal.pone.0070986.

Nwankwo, C.C., Okpokwasili, G., 2019. Molecular characterization of microorganisms in crude oil-polluted mangrove swamps of the Niger Delta, Rivers State, Nigeria. J. Bioremediation Biodegrad 10, 1–11.

Qin, L., Tian, P., Cui, Q., Hu, S., Jian, W., Xie, C., Yang, X., Shen, H., 2021. Bacillus circulans GN03 alters the microbiota, promotes cotton seedling growth and disease resistance, and increases the expression of phytohormone synthesis and disease resistance-related genes. Front. Plant Sci. 12. https://doi.org/10.3389/fpls.2021.644597.

Radakovits, R., Jinkerson, R.E., Fuerstenberg, S.I., Tae, H., Settlage, R.E., Boore, J.L., Posewitz, M.C., 2012. Draft genome sequence and genetic transformation of the oleaginous alga Nannochloropsis gaditana. Nat. Commun. 3, 686. https://doi.org/10.1038/ncomms1688.

Rafeeq, H., Afsheen, N., Rafique, S., Arshad, A., Intisar, M., Hussain, A., Bilal, M., Iqbal, H.M.N., 2023. Genetically engineered microorganisms for environmental remediation. Chemosphere 310, 136751. https://doi.org/10.1016/j.chemosphere.2022.136751.

Rajabi, H., Mosleh, M.H., Mandal, P., Lea-Langton, A., Sedighi, M., 2020. Emissions of volatile organic compounds from crude oil processing – Global emission inventory and environmental release. Sci. Total Environ. 727. https://doi.org/10.1016/j.scitotenv.2020.138654.

Rehm, H.J., Reiff, I., 1981. Mechanisms and occurrence of microbial oxidation of long-chain alkanes BT - Reactors and Reactions. In: Advances in Biochemical Engineering. Springer Berlin Heidelberg, Berlin, Heidelberg, pp. 175–215.

Rodrigues, C.J.C., de Carvalho, C.C.C.R., 2022. Cultivating marine bacteria under laboratory conditions: overcoming the "unculturable" dogma. Front. Bioeng. Biotechnol. 10. https://doi.org/10.3389/fbioe.2022.964589.

Rojo, F., 2009. Degradation of alkanes by bacteria: Minireview. Environ. Microbiol 11, 2477–2490. https://doi.org/10.1111/j.1462-2920.2009.01948.x.

Saadoun, I.M.K., 2015. Impact of Oil Spills on Marine Life. In: Larramendy, M.L., Soloneski, S. (Eds.), Emerging Pollutants in the Environment. IntechOpen. https://doi.org/10.5772/60455.

Sabirova, J.S., Ferrer, M., Regenhardt, D., Timmis, K.N., Golyshin, P.N., 2006. Proteomic insights into metabolic adaptations in Alcanivorax borkumensis induced by alkane utilization. J. Bacteriol. 188, 3763–3773. https://doi.org/10.1128/JB.00072-06.

Sakshi, Singh, S.K., Haritash, A.K., 2021. Catabolic enzyme activity and kinetics of pyrene degradation by novel bacterial strains isolated from contaminated soil. Environ. Technol. Innov. 23, 101744. https://doi.org/10.1016/J.ETI.2021.101744.

Sakshi, Singh, S.K., Haritash, A.K., 2023. Bacterial degradation of mixed-PAHs and expression of PAH-catabolic genes. World J. Microbiol. Biotechnol. 39, 1–13. https://doi.org/10.1007/s11274-022-03489-w.

Sarsaiya, S., Kumar, S., Kumar, M., Kumar, A., Mishra, S., Chen, J., 2017. Bioresource Technology The dynamic of cellulase activity of fungi inhabiting organic municipal solid waste. Bioresour. Technol. 0–1. https://doi.org/10.1016/j.biortech.2017.12.011.

Shinoda, Y., Sakai, Y., Uenishi, H., Uchihashi, Y., Hiraishi, A., Yukawa, H., Yurimoto, H., Kato, N., 2004. Aerobic and anaerobic toluene degradation by a newly isolated denitrifying bacterium, thauera sp. Strain DNT-1. Appl. Environ. Microbiol 70, 1385–1392. https://doi.org/10.1128/AEM.70.3.1385-1392.2004.

Silliman, B.R., Koppel, J., Van De, McCoy, M.W., Diller, J., Kasozi, G.N., Earl, K., Adams, P.N., Zimmerman, A.R., 2012. Degradation and resilience in louisiana salt marshes after the bp-deepwater horizon oil spill. Proc. Natl. Acad. Sci. U. S. A. 109, 11234–11239. https://doi.org/10.1073/pnas.1204922109.

Srivastava, S., Dafale, N.A., 2024. Genomic dissection of Niallia sp. for potential application in lignocellulose hydrolysis and bioremediation. Arch. Microbiol 206, 1–11. https://doi.org/10.1007/s00203-023-03728-0.

Tamura, K., Stecher, G., Kumar, S., 2021. MEGA11: molecular evolutionary genetics analysis version 11. Mol. Biol. Evol. 38, 3022–3027. https://doi.org/10.1093/molbev/msab120.

Viñas, M., Grifoll, M., Sabaté, J., Solanas, A.M., 2002. Biodegradation of a crude oil by three microbial consortia of different origins and metabolic capabilities. J. Ind. Microbiol. Biotechnol. 28, 252–260. https://doi.org/10.1038/sj/jim/7000236.

Wang, D., Lin, J., Lin, J., Wang, W., Li, S., 2019. Biodegradation of petroleum hydrocarbons by bacillus subtilis BL-27, a strain with weak hydrophobicity. Molecules 24. https://doi.org/10.3390/molecules24173021.

Wang, M., Ding, M., Yuan, Y., 2023. Bioengineering for the microbial degradation of petroleum hydrocarbon contaminants. Bioengineering 10. https://doi.org/10.3390/bioengineering10030347.

Wang, S., Li, G., Liao, Z., Liu, T., Ma, T., 2022. A novel alkane monooxygenase (alkB) clade revealed by massive genomic survey and its dissemination association with IS elements. PeerJ 10. https://doi.org/10.7717/peerj.14147.

Wang, W., Shao, Z., 2013. Enzymes and genes involved in aerobic alkane degradation. Front. Microbiol 4, 1–7. https://doi.org/10.3389/fmicb.2013.00116.

Xu, X., Liu, W., Tian, S., Wang, W., Qi, Q., Jiang, P., Gao, X., Li, F., Li, H., Yu, H., 2018. Petroleum hydrocarbon-degrading bacteria for the remediation of oil pollution under aerobic conditions: a perspective analysis. Front. Microbiol 9, 1–11. https://doi.org/10.3389/fmicb.2018.02885.

Yakimov, M.M., Bargiela, R., Golyshin, P.N., 2022. Calm and Frenzy: marine obligate hydrocarbonoclastic bacteria sustain ocean wellness. Curr. Opin. Biotechnol. 73, 337–345. https://doi.org/10.1016/J.COPBIO.2021.09.015.

Yilmaz, E.I., 2003. Metal tolerance and biosorption capacity of Bacillus circulans strain EB1. Res. Microbiol 154, 409–415. https://doi.org/10.1016/S0923-2508(03)00116-5.

Ying, J., Ye, J., Xu, T., Wang, Q., Bao, Q., Li, A., 2019. Comparative Genomic Analysis of Rhodococcus equi: An Insight into Genomic Diversity and Genome Evolution.

Yu, J., Cai, W., Zhao, S., Wang, Y., Chen, J., 2013. Aerobic biodegradation of chlorinated hydrocarbons by bacillus circulans WZ-12 CCTCC M 207006 under saline conditions. Chin. J. Chem. Eng. 21, 781–786. https://doi.org/10.1016/S1004-9541(13)60536-4.

Zheng, C., He, J., Wang, Y., Wang, M., Huang, Z., 2011. Hydrocarbon degradation and bioemulsifier production by thermophilic Geobacillus pallidus strains. Bioresour. Technol. 102, 9155–9161. https://doi.org/10.1016/j.biortech.2011.06.074.

Zhong, C., Zhao, J., Chen, W., Wu, D., Cao, G., 2020. Biodegradation of hydrocarbons by microbial strains in the presence of Ni and Pb. 3 Biotech 10, 1–11. https://doi.org/10.1007/s13205-019-2011-2.